Designing Copper-Amino Acid Based BioMOFs for Enzyme Mimetic Applications

M.Sc. Thesis

By

AAYUSHI BIYANI

DEPARTMENT OF CHEMISTRY

INDIAN INSTITUTE OF TECHNOLOGY

INDORE

MAY,2024

Designing Copper-Amino Acid Based BioMOFs for Enzyme Mimetic Applications

A THESIS

Submitted in partial fulfilment of the
requirements for the award of the degree
of

Master of Science

by

AAYUSHI BIYANI

DEPARTMENT OF CHEMISTRY

INDIAN INSTITUTE OF TECHNOLOGY INDORE

MAY,2024

INDIAN INSTITUTE OF TECHNOLOGY, INDORE

CANDIDATE'S DECLARATION

I hereby certify that the work which is being presented in the thesis entitled as **Designing Copper-Amino Acid Based BioMOFs for Enzyme Mimetic Applications** in the partial fulfilment of the requirements for the award of the degree of **MASTER OF SCIENCE** and submitted in the **DISCIPLINE OF CHEMISTRY, Indian Institute of Technology Indore**, is an authentic record of my own work carried out during the time period from July 2023 to May 2024 under the supervision of Dr. Tridib Kumar Sarma Associate professor, Department of Chemistry, IIT Indore.

The matter presented in this thesis has not been submitted by me for the award of any other degree of this or any other institute.

Aayushi 07/05/24

Signature of the Student (with date)

AAYUSHI BIYANI

This is to certify that the above statement made by the candidate is correct to the best of my knowledge.

07-05-2024

Signature of the Supervisor of M.Sc. Thesis (with date)

Dr. TRIDIB KUMAR SARMA

AAYUSHI BIYANI has successfully given her M.Sc. Oral Examination held on 08/05/2024.

Signature(s) of Supervisor(s) of MSc thesis

Dr. Tridib Kumar Sarma

Date: 08-05-24

Signature(s) of Convenor, DPGC

Dr. Umesh A. Kshirsagar

Date: 24.05.2024

Signature of PSPC Member 1

Prof. Sanjay Kumar Singh

Date: 8/5/24

Signature of PSPC Member 2

Dr. Satya S. Bulusu

Date:

ACKNOWLEDGEMENT

I am profoundly grateful for the consistent guidance and support provided by Dr. Tridib Kumar Sarma, my supervisor, throughout this project. Collaborating with him has been exceptionally rewarding, offering me the opportunity to tackle various challenges and grasp essential concepts pivotal to my research. His invaluable advice and encouragement regarding my future academic endeavors have been deeply cherished.

I extend my heartfelt appreciation to the members of the chemistry department faculty, particularly Prof. Sanjay Kumar Singh and Dr. Satya S. Bulusu, my PSPC guides, for their diverse assistance. The timely technical support from the department staff and the essential resources provided by the Sophisticated Instrumentation Centre (SIC) at IIT Indore have played a crucial role in facilitating my research. For XPS analysis, I would really like to thank SAPTRISHI, IIT Jammu.

A special acknowledgment goes to Mr. Aditya Prasun, my mentor, whose continuous guidance and insightful suggestions have been indispensable throughout this project.

I also want to express gratitude to my fellow lab mates—Ms. Amrita, Ms. Vidhi, Mr. Tarun, Mr. Surya Kamal, Mr. Ravindra, Mr. Yonas, Mr. Rahul Mr. Debanjan, Ms. Huma, Ms. Priyanka, Mr Khushwant, Mr. Sachin, Mr. Naveen, and Mr. Suman—for their assistance in both academic and non-academic matters. I am sincerely thankful to all my batchmates and friends for their unwavering support.

Lastly, I convey my deepest love and gratitude to my beloved parents, Mr. Manoj Kumar Biyani and Mrs. Sunita Manoj Biyani, and my siblings for their unconditional love and unwavering support.

AAYUSHI BIYANI

Dedicated to

My Beloved Family

ABSTRACT

The use of natural biomolecules with multiple coordination sites can be a greener alternative to the synthetic ligands utilized to fabricate metal-organic frameworks (MOFs). Conventional synthetic ligands suffer from tedious synthesis procedures and poor biocompatibility. Natural biomolecules such as amino acids, nucleobases, polyphenols, sugar, *etc.*, however, are earth-abundant and eco-friendly. Such biomolecules, when complexed with suitable metal ions, can inherit/enhance their intrinsic medicinal/chemical properties. Amino acids can coordinate with different transition metal ions to produce materials that are employed in various applications. Enzyme-mimicking is one common application used for such metal-amino acid-based materials. Copper (II)-amino acid interactions are widely studied in literature. However, no reports are present discussing interaction of Cu(I) ions with amino acids. Herein, we developed a greener route to synthesize amino acid-capped CuI microcrystals that showed excellent peroxidase like activities. These enzyme-mimics maintain their activities in wide pH and temperature range. Apart from enzyme-mimic, synthesized microcrystals can also be employed in various applications known for CuI-based materials.

Table of Contents

LIST OF FIGURES

LIST OF TABLES

SCHEMES

ACRONYMS

MOFs	Metal Organic Frameworks
CuI	Copper Iodide
BioMOFs	Metal Biomolecule Frameworks
HSAB	Hard Soft Acid Base
CO_2	Carbon dioxide
ROS	Reactive Oxygen Species
TE	Thermoelectric
AA	Aspartic acid
TEM	Transmission Electron Microscopy
H_2O_2	Hydrogen Peroxide
DI	Deionized
rpm	Rotation per minute
RB Flask	Round Bottom Flask
rt	Room temperature
λ_{ex}	Excitation wavelength
λ_{em}	Emission wavelength
BE	Binding Energy
K_m	Michaelis Constant
V_{max}	Maximum Velocity
V_o	Initial reaction rate
S_o	Substrate concentration
TA	Terephthalic Acid
HRP	Horseradish Peroxidase
DTA	Differential thermal analysis

FESEM	Field emission scanning electron microscopy
FTIR	Fourier Transform Infrared
EDX	Energy Dispersive X-ray Spectroscopy
TGA	Thermogravimetric Analysis
APS	Ammonium persulfate
LAA	L-aspartic acid
POM	Polarized electron microscope
PXRD	Powder X-ray Diffraction
BET	Brunauer- Emmet Isotherm
NPs	Nanoparticles
XPS	X-ray Photoelectron Spectroscopy
UV-Vis	Ultraviolet-Visible
CD	Circular Dichroism
TMB	3,3’5,5’-tetramethylbenzidine
OxTMB	Oxidized 3,3’5,5’-tetramethylbenzidine
AB-RT	Sample code
AB-RTS	Sample code
CLA-16	Sample code
CGA-16	Sample code
CTA-16	Sample code
CCA-16	Sample code
CHA-16	Sample code
CglA-16	Sample code
CAlA-16	Sample code

NOMENCLATURE

°C: - Degree centigrade

Pa: - Pascal

g: - Gram

mg: - Milligram

µL: - Microliter

mL: - Milliliter

mM: - Millimolar

min: - minute

M: - Molar

µm: - Micrometer

eV: - electron Volt

%: - Percent

s: - Seconds

K: - Kelvin

Chapter 1

Introduction

Metal complexes with organic molecules (termed as ligands) are long known in the literature. Such materials are recognized by names like metal- organic frameworks, coordination polymers, and organic zeolite analogues *etc.* MOFs are compounds containing repeating coordination entities that consists of inorganic metal ions (having empty orbitals) or cluster of metal ions and organic ligands (lone pair containing) linked by coordinate bonds, which results in extended networks in one, two, and three dimensions. High surface area, good adsorption capacity, enriching surface functionality, structural tailorability and accommodable pore size, *etc.* properties owe to MOFs wide applicability in chemical and biological applications.[1] Besides enthralling properties of MOFs, real life applications are still restricted due to certain adverse environmental effect of the orthodox synthesis approaches. In conventional synthesis of MOF, typically synthetic organic ligands and organic solvents are used which are punitive for the environment. As most of the synthetic organic ligands suffer from severe drawbacks (sophisticated and tedious reaction procedures, toxic and carcinogenic precursors and solvents, costly chemicals, *etc.*), researchers felt an urgent need to find a greener alternative. Thus, to form biologically and environmentally compatible MOFs, safer solvents, sustainable metal ion and biocompatible organic ligand should be used. Since biomolecules have many advantages such as they are naturally abundant, structurally diverse, have different metal binding sites, can show intrinsic self-assembly properties and most importantly they are biocompatible.[2] Consequently, various scientists started exploring naturally abundant biomolecules such as amino acids, peptides, nucleobases, and saccharides to serve as organic ligand. This subcategory of MOFs, utilizing biomolecules as organic ligands is often termed as Metal-Biomolecule Frameworks).[3] Biomolecules mentioned earlier, encompass variety of functional groups and multiple coordination sites which can be beneficial in the case of catalysis, enantioselective synthesis, separation, and CO_2 capture.[4]

Amino acids are the elementary biological units, The term amino acid are molecules having amine and carboxylic group attached to carbon atom. The simplest amino acid is known as glycine. Other common amino acids have side chains (symbolized by R)

substituted on the carbon atom. Amino acids are linked via amide bonds to form peptides and proteins that have various biological functions. Amino acids, depending on their side chain, can act as mono-, bi-, or multidentate ligands to coordinate with the metal ions.[5]

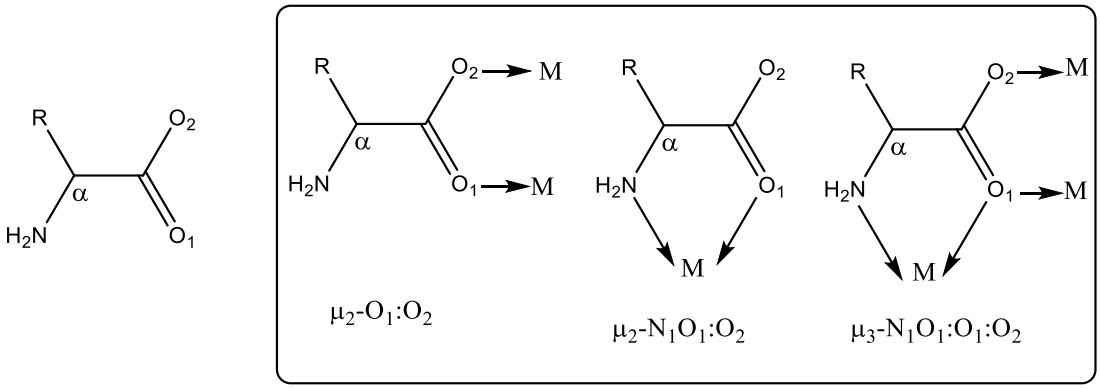

Figure 1. *Schematic diagram of the common skeleton of a natural amino acid and their potential coordination modes.*

Lately, numerous reports employing amino acids as a ligand with range of main group and transition metal ions to fabricate various functional materials are abundant in the literature. Such amino acids-based Biomaterials are being used in various applications such as catalysis, enantioselective synthesis, separation, CO_2 capture and drug delivery.[6]

All biological processes are very slow, thus require a catalyst to enhance the reaction rate to make life feasible. Nature has fascinatingly designed specific biocatalysts for specific biochemical reaction. These specific biocatalysts are known as 'Enzymes'. Enzymes are usually extremely complex protein structures where the active site may or may not contain a metal ion. Enzymes, as already discussed are specific for a reaction, and operate within optimum reaction conditions (physiological). In 20th century, to utilize the specificity of enzymes to get specific single product, enzymes were introduced into industries. Soon after, it was realized that these biocatalysts suffer from drawbacks. To provide an alternate to enzymes in the industries, synthetic enzymes were fabricated, which suffered from tedious synthetic procedures, tiresome purification process, and extremely high cost. Enzyme mimicking refers to the ability of certain molecules or materials to mimic the function of natural enzymes. Enzyme mimics, also known as artificial enzymes, that are not proteins but can perform similar

catalytic functions to natural enzymes. They mimic the binding and catalytic sites of natural enzyme. Enzyme mimics should have less complex structure than their natural counterparts, lower molecular weight and higher stability than their naturally occurring enzymes. Enzyme mimics have certain advantages over natural enzymes such as tunable structure, lower cost, excellent tolerance to vigorous experimental conditions, easy synthetic routes, and better solubility in most solvents. There are many types of enzyme mimics that have been synthesised such as polymeric and dendrimeric enzyme mimics, supramolecular enzyme mimics and proteinic (protein and antibody) enzyme mimics. Enzyme mimics has several applications such as in biological reactions, biosensors, medical uses, green and sustainable chemistry, antibiofouling and for production of biofuel.[6]

In biological systems, presence of various metal ions is well known. Many transition metal ions such as Fe, Mn, Cu, Zn, *etc.* serve crucial role in catalysing many biochemical processes. These metal ions are present at the active sites of the biocatalysts (enzymes) where they are coordinated to specific amino acids of the proteins which is responsible for their catalytic activity. Copper is found in all living organisms and is important for the functioning of several enzymes *e.g.*, cytochrome oxidase, superoxide dismutase, ascorbate oxidase, and tyrosinase. Thus, scientists have fabricated various frameworks consisting of amino acids with copper. Copper is found in all living organisms and is important for the functioning of several enzymes such as cytochrome c-oxidase, laccase, ascorbate oxidase, superoxide dismutase and tyrosinase. Copper ions (in the forms of Cu(I) and Cu (II)) play a significant role as cofactors in a variety of natural enzymes.[7]

Copper(I) have stable electronic configuration $3d^{10}4s^{0}$. As per HSAB principle, Cu^{+} is a soft acid and I^{-} is softer base as compare to Cl^{-} and Br^{-}. Therefore, CuI is the more stable compound in comparison to CuBr and CuCl. Copper iodide acts as a reducing agent because it can easily oxidize iodide to iodine. It has very poor solubility in water and ethanol but can be solubilized in liquid ammonia, dilute hydrochloric acid, potassium iodide, potassium cyanide and sodium thiosulfate solution. CuI shows good solubility in acetonitrile. Thanks to the rich coordination chemistry of copper iodide, it can form structurally diverse molecular complexes and extended coordination networks when combined with various organic and inorganic ligands. These coordination

networks can display a wide-ranging physical and chemical properties such as electroluminescence, photocatalysis, electrical conductivity, and sensing.[8]

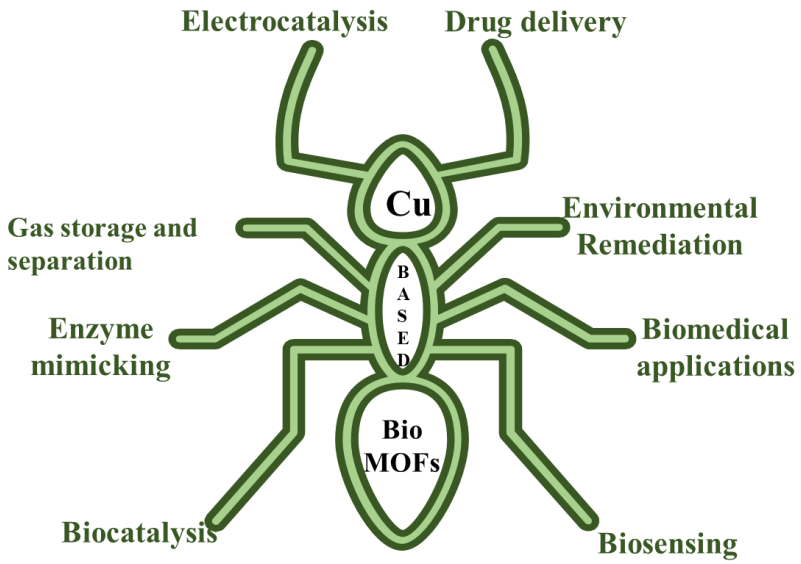

Figure 2. *Applications of Cu-based materials.*

CuI is a semiconductor material having bandgap (3.1 to 3.2 eV) and crystal structure suitable for photochromic applications.[9] As nanoparticles, CuI shows enhanced luminescent properties compared to its bulk form, including different emission wavelengths, higher intensity, and improved stability. Due to their luminescent properties, CuI nanoparticles can be used in various applications such as optoelectronic devices, light-emitting diodes (LEDs), photodetectors, and bioimaging.[10] Surface modifications or doping with other elements can enhance the luminescent properties and stability of CuI nanoparticles. Due to above mentioned properties of CuI can be an excellent choice to develop an enzyme mimic.

Chapter-2

Literature Survey

Metal organic frameworks, despite having various exceptional properties and wide applicability, have certain limitations that limit their use on a larger scale mainly in biological applications. The introduction of biomolecules as a ligand has helped in overcoming most of the drawbacks associated with conventional MOFs. In recent years, many BioMOFs have been reported in the literature utilizing several modified/natural biomolecules (amino acids, peptides, nucleobases, sugars, *etc.*) with a wide range of metal ions, for diverse applications. Amino acids, due to the presence of multiple functional groups, are extensively explored to fabricate multidimensional frameworks.

Wang et.al fabricated a zirconium-based MOF, MIP-202(Zr). Aspartic acid was used as a ligand as it is the smallest amino acid bearing two carboxylate groups in a distance suitable to form chelate with metal ions. Unlike other Zr-based MOFs synthesis of this material was green, as the synthesis procedure consisted of simple stirring for a long time with the use of water as solvent. This MOF, due to some characteristic features viz. easily accessible NH_3^+ group, porous tunnel-like channels in the crystal structure, and extremely high hydrolytic stability was assumed to be an excellent proton conductor. As per assumption, MOF has shown extremely high proton conduction at 363K and under 95% relative humidity. Further, the MOF shows good chemical stability, and it is very cost-effective.[11]

Mon et al synthesized a novel porous chiral bioMOF using non-toxic metals Calcium and Copper with modified aspartic acid as a ligand. Aspartic acid was modified with thionyl chloride to make a proligand. The aqueous solution of this proligand was then added to an aqueous solution consisting of metal ions to form crystals of the bioMOF. SCXRD structure analysis confirmed a porous structure. This network was then used to encapsulate dopamine and act as a drug delivery agent as it degrades in physiological acidic conditions.[12]

Among various reported MOF systems, Copper ions-based MOFs have attracted the special attention of researchers as copper ions are extensively present in biological

systems. Cu is present in many enzymes such as cytochrome c-oxidase, peroxidase, amine oxidase, nitrite reductase and tyrosinase. Thus, plenty of work has already been done to fabricate BioMOFs having copper as metal centre. Some of the reported Cu based BioMOFs are as follows-

Gizer et.al synthesised a MOF having L-Aspartic acid as a ligand and different sources of Cu (II) ion such as acetate, sulfate, nitrate and chloride as the metal centre to synthesise respective BioMOFs via a green route using water as solvent. In their BioMOF Cu(II) ions are coordinating with carboxylic acid group of L-Aspartic acid and form rod like assemblies with hexagonal crystallisation patterns. Synthesised BioMOFs were checked for their glucosidase inhibiting capability, antimicrobial activity and hemocompatibility test. In this way they have designed BioMOF using biocompatible and renewable precursors having high porosity and internal surface area which will be a greener and more suitable alternative for various industrial and biomedical applications.[13]

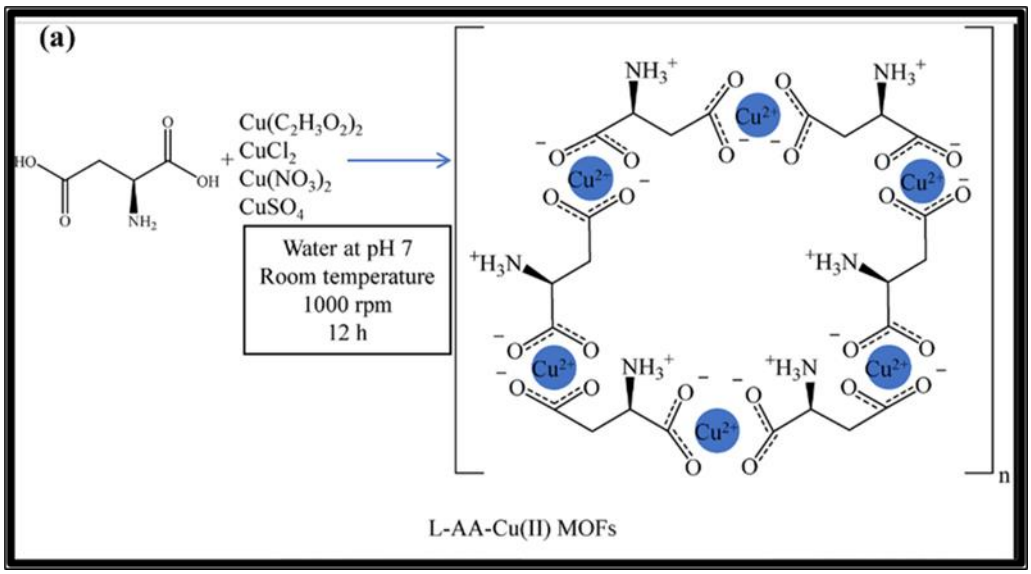

Figure 3 *Schematic representation of L-Aspartic acid-based MOF synthesis*[13]

In a related instance, Liu *et al.* (2022) detailed the development of a copper aspartic acid (CuAsp) metal-organic framework (MOF) where aspartic acid serves as a ligand, coordinating with the metal centre via both amino and two carboxylate groups. This fibrous CuAsp MOF exhibited NADH-peroxidase and glycerol dehydrogenase (GlyDH) mimicking activities. The resultant nanozyme displayed notably heightened catalytic efficacy across a broad spectrum of pH levels, temperatures, and solvent environments compared to the free enzyme. Moreover, the synthesized nanozyme

showcased enhanced stability, retaining its original activity even after a month-long storage period. This breakthrough underscores the expanded application potential of BioMOFs in the realm of biocatalysis.[14]

Surprisingly, interaction between Copper(I) and amino acids is not present in literature. However, Cu(I) based materials exhibits various unique and interesting properties that are crucial for various industrial and pharmaceutical applications.

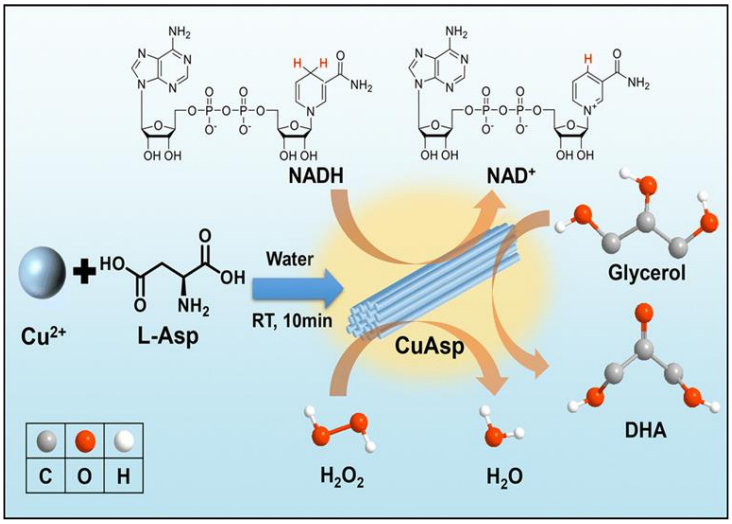

Figure 4. *Schematic representation of the preparation of CuAsp for catalytic oxidation of NADH dehydrogenase and glycerol in the presence of* H_2O_2.[14]

Ravaro *et al.* conducted an analysis of a new luminescent copper (I) complex, $CuI(PPh_3)$(4,4′-dimethoxy-2,2′-bipyridine), displaying interesting solvatochromic properties. The orange-coloured complex, when recrystallized from acetonitrile, changes to yellow showcasing a blue-shifted emission spectrum. This modification can be overturned when the yellow solid is recrystallized in dichloromethane. The observed colour change is attributed to the distorted molecular packing of the complex in its solid state.[15] Wang *et al.* A highly luminescent ink has been developed using a hybrid cluster composed of copper-iodide and 1-Propyl-1,4-diazabicyclo [2.2.2] octan-1-ium ($Cu_4I_6(pr\text{-}ted)_2$), achieving a quantum efficiency of over 98%. Through the interaction between the cluster and polyvinylpyrrolidone (PVP), a highly luminescent ink is easily produced via a one-pot solution process. This ink is utilized to create an anti-counterfeiting image and produce a uniform film, demonstrating its potential application in light-sensitive compound (LSC) devices.[16] Almasoudi *et al.* developed a highly transparent thin films of γ-CuI with improved thermoelectric (TE) properties

that, after annealing at high temperature, led to the evaporation of iodine. It reduced deviations from the stoichiometric composition that showed optimal TE performance (power factor 1600 μW/(m K^2) at 300 K). Additionally, this film displayed low thermal conductivity.[17] Li *et al.* made-up a system in which CuI is homogeneously coated on carbon cloth (CuI@CC) using electroplating deposition followed by iodination procedure at ambient temperature. Combined effect of flexibility (from the carbon fiber) and excellent adsorptive ability (CuI coating), the CuI@CC acts as flexible, efficient, self-cleaning, and easy-recycling adsorbent towards cationic organic dyes with excellent repeatability. Remarkably, the CuI coating is also self-cleaning to decompose adsorbed organics through photocatalysis.[18] Pramanik *et al.* synthesized CuI nanoparticles of an average size of 8 nm using a co-precipitation method,.These nanoparticles are effective against both gram-positive and gram-negative bacteria. It is believed that the CuI NPs generate reactive oxygen species (ROS) in both types of bacteria, leading to ROS-mediated DNA damage that inhibits transcription, as shown by reporter gene assays. The potential antibacterial mechanisms of the CuI NPs include ROS-induced DNA damage and membrane ruptures. Copper iodide nanoparticles (CuI NPs) have garnered significant interest among synthetic chemists due to their beneficial qualities. These include high atom economy, cost-effectiveness, ease of synthesis, accessibility, and the catalyst's reusability.[19] Li *et al.* formed a Cu-CuI composite catalyst containing an abundance of Cu/Cu+ interfaces by physically mixing Cu nanoparticles and CuI powders. This composite catalyst achieves an impressive C_{2+}. The Cu-CuI composite's high-rate C_{2+} production is attributed to the presence of residual Cu^{+} and adsorbed iodine species. These components enhance CO adsorption thus promoting C-C coupling. The electrochemical reduction of CO_2 to multicarbon hydrocarbons and oxygenates (C_{2+}) is crucial due to its high energy density and abundance. This process offers a promising path to enable renewable energy storage and close the carbon cycle.[20]

Copper ions can have different redox states *i.e.* oxidized Cu (II) or reduced (I), due to which these ions play a crucial role in cell physiology and enzyme activity. Copper in its +1 state, is used as a catalyst in various pharmaceutically important organic transformations. Due to presence of copper in natural enzymes and its ability to exist in more than one oxidation state drew attention of researchers for developing enzyme-mimic with Cu as central metal ion. Copper-based enzyme-mimicking materials are

widely present in literature. For example, Yang *et al.* devised a binuclear Cu_2(μ-6-benzylaminopurine)$_4$.$2H_2O$ BioMOF through an acid-base synthesis route, employing Cu (II) as the central metal and a plant growth regulator as the organic ligand. The resulting deprotonated binuclear BioMOF demonstrated exceptional stability within alkaline environments and exhibited remarkable peroxidase mimicking capabilities. Unlike conventional Cu-based peroxidase mimics, this BioMOF directly catalyses the hydrolysis of H_2O_2 into O^{2-} without generating OH free radicals, ultimately degrading into its initial synthetic precursors. Further, a hybrid nanomaterial, namely BioMOF-NPs, was formed by integrating BioMOF with chitosan nanoparticles. This hybrid material demonstrated reliable and repeatable H_2O_2 scavenging efficacy, showcasing promising potential for cyclic utilization.[21]

In 2020, our group synthesize copper vanadate nanoribbons by hydrothermal process, which can efficiently mimic the activity of multiple enzymes such as peroxidase, oxidase, and laccase enzymes (Figure 5). 26 As a practical application, these copper vanadate nanoparticles have been utilized in the field of biosensing for the detection of epinephrine and glutathione. Kinetics studies show that the catalyst has high catalytic efficiency with very low Km values. Overall, the study provides insights into the use of copper vanadate nanoribbons as nanozyme for biosensing applications. [22]

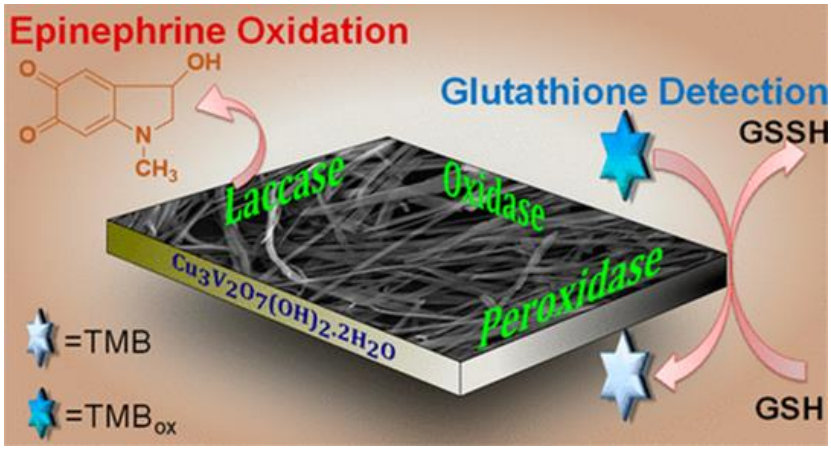

Figure 5. *Excellent multienzymatic activity of Copper Pyrovanadate Nanoribbons.*[22]

Wu *et al.* synthesized functional molecules by utilizing a self-assembly approach that combines inorganic salts and amino acids. Their method magnificently formed nanoflowers using copper (II) ions and natural amino acids under gentle conditions. The study reveals that the interactions between amino acids and copper ions drive the

formation of nanoflowers. These nanoflowers contain copper ions and Cu (AA)n complexes with Cu-O bonds, contributing to their structure. The nanoflowers feature a flower-like, porous architecture primarily influenced by the amino acids' R groups, offering a high surface-to-volume ratio that enhances their peroxidase-like activity through a Fenton-like reaction.[23]

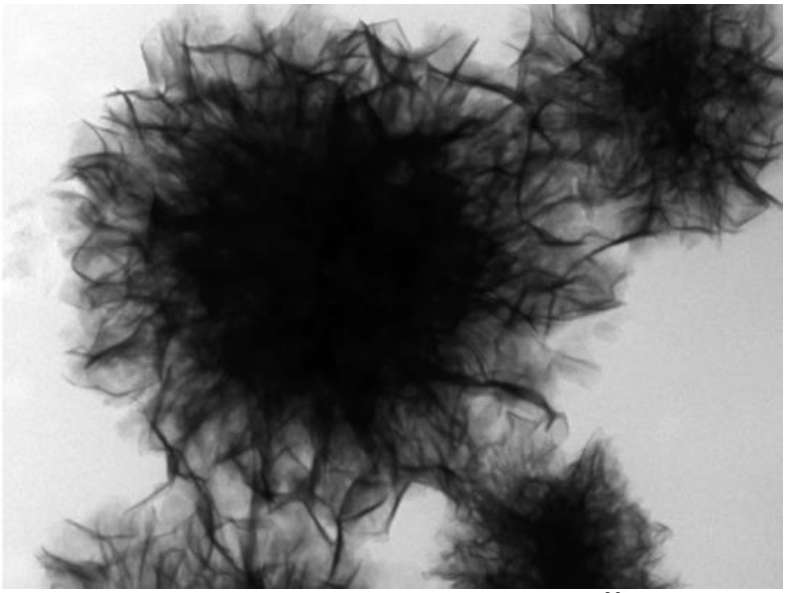

Figure 6. *TEM of the hybrid organic–inorganic nanoflower.*[23]

Objective of the Work

Based on literature reports discussed earlier, it is obvious that interaction between amino acids and Cu (II) ions is well-explored. Cu-amino acids-based materials are known to show impressive enzyme-mimicking behaviour. However, no reports are present in the literature studying interaction between amino acids with Cu(I) ions. Therefore, following objectives were designed for our work:

1. To utilize Cu(I) compounds and amino acids as building blocks for the development of novel BioMOFs/materials.
2. Study the interaction between Cu(I) and amino acids using various analytical and spectroscopic techniques.
3. Explore synthesized materials as a potential enzyme-mimic.

Chapter 3

Experimental Section

3.1. Reagents and Chemicals

Copper iodide (Sigma), Glutamic acid (Merck specialties Pvt. Ltd.), D-Aspartic acid (Spectrochem Pvt. Ltd.), L-Aspartic acid (HiMedia laboratories Pvt. Ltd.), Copper acetate (Spectrochem Pvt. Ltd.), Ammonium per sulfate (Sisco research laboratories Pvt. Ltd), Sodium hydroxide (Merck Pvt. Ltd.), Disodium hydrogen phosphate (Hi Media Pvt. Ltd.), Sodium dihydrogen phosphate (Hi Media Pvt. Ltd.), Copper sulfate (Sigma), Copper bromide (Sigma), Copper chloride (Sigma), Tryptophan (Sisco research laboratories Pvt. Ltd), Citric Acid (Sisco research laboratories Pvt. Ltd), Ascorbic Acid (Sisco research laboratories Pvt. Ltd), Histidine (Sisco research laboratories Pvt. Ltd), Hydrogen Peroxide (AVRA synthesis Pvt Ltd), Glycine (Sisco research laboratories Pvt. Ltd), Alanine (Sisco research laboratories Pvt. Ltd), Sodium acetate trihydrate (Merck specialties Pvt. Ltd.), TMB (Sigma), and Terephthalic acid (Sisco research laboratories Pvt. Ltd).All the chemicals were used without further purifications.

3.2. Instrumentation and Methods

Perkin Elmer's spectrum II instrument was utilized to measure FTIR spectra in the 4000-400 cm^{-1} range with a 4 cm^{-1} resolution having 1 sec intervals. The morphology of the CLA-16 and other materials were obtained using a Supra55 Zeiss field emission scanning electron microscope (FE-SEM). A Rigaku Smartlab instrument having Cu Kα source (X-ray wavelength of 0.154 nm) was used to record the Powder X-ray diffraction (PXRD) pattern. Thermal stability was determined by Mettler Toledo TGA/DSC 1 thermogravimetric analyser. Almicro Ore trinocular microscope OR02 was used to take polarized optical images of the synthesized samples. X-ray photoelectron spectroscopy (XPS) data was collected using a Thermoscientific NEXSA Surface analyzer. The Brunauer-Emmett-Teller (BET) surface area was determined using an Autosorb iQ2 instrument by Anton Paar Quantachrome. Enzymatic activity of CLA-16 was monitored by recording UV-Visible spectra with a PerkinElmer Lambda 750 UV Spectrometer. For Circular Dichroism measurements, JASCO J-815 spectropolarimeter was used. Fluorescence measurements were performed on Horiba Fluoromax-4. Zeta potential measurements were performed on Micromeritics Nanoplus-3.

3.3 Using Cu(I) metal salts and L-Aspartic acid as precursors

In literature, significant reports are present showing high affinity of copper and aspartic acid to readily form multidimensional structures. Taking advantage of this known chemistry, attempts were made to use Cu(I) salts instead of Cu(II). These reactions were carried out at room temperature (**Scheme 1**) and at elevated temperature (**Scheme 2**).

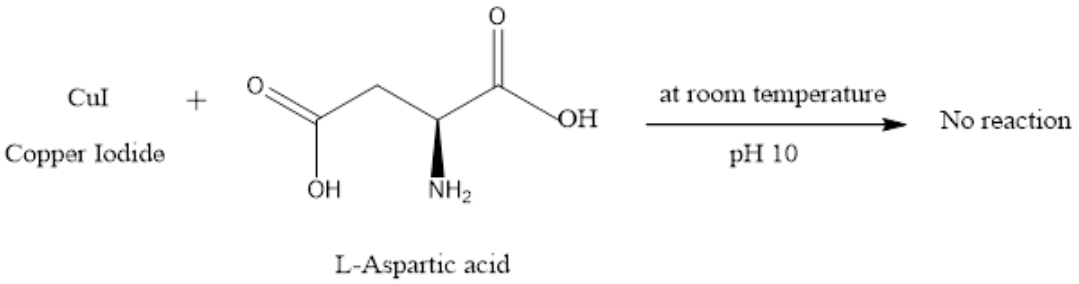

Scheme 1. *Schematic representation of reaction between CuI and L-AA at pH=10 in aqueous conditions*

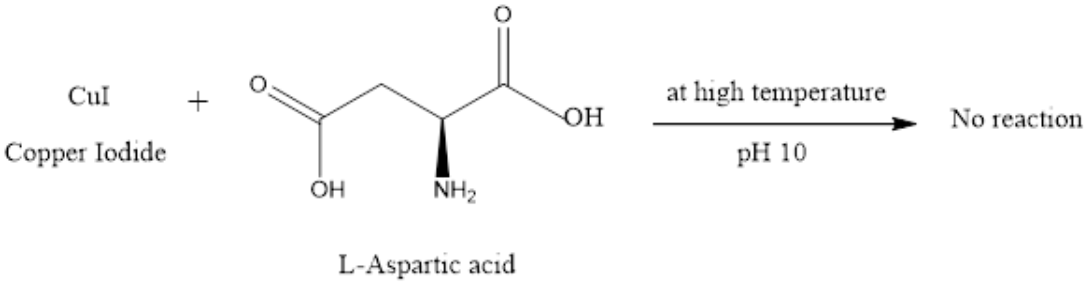

Scheme 2. *Schematic representation of reaction between CuI and L-AA at pH=10 in aqueous conditions*

In above mentioned reactions, small amount of precipitate was observed. After characterizing it, no interactions between amino acid and metal were observed. The possible reason behind the observation was solubility of copper iodide in water. It is well-known that Cu(II) salts are soluble in water. Thus, to take advantage of this fact, a mild oxidizing agent ammonium persulfate was introduced in the system to partially oxidize the Cu(I) ions to Cu(II).

3.4. Synthesis of AB-RT

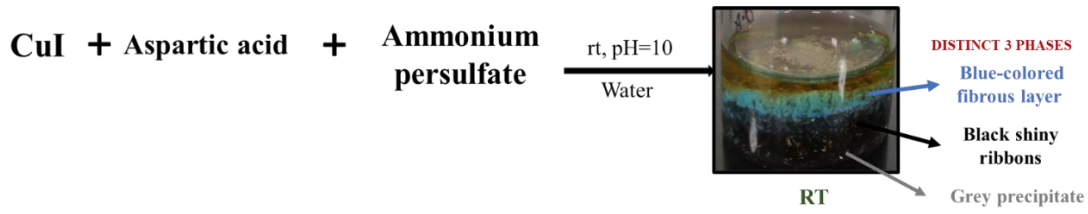

Scheme 3. *Schematic representation of Synthetic procedure of AB-RT*

Procedure-

In a typical procedure, 50 Mm of L-aspartic acid was added in a 15 mL glass vial having 10 mL water. The solution pH was adjusted to 10 using 1M NaOH solution. This solution was then kept on constant stirring for few minutes to assure complete dissolution of amino acid. 50 mM CuI was added to the above solution followed by the addition of 100 mM ammonium persulfate. The resultant solution was then kept undisturbed. After a few hours of addition, three distinct phases (**Scheme 3.)** were observed. Many efforts were made to separate all three phases, however, due to the unstable nature of these phases no separation was possible.

3.5. Synthesis of AB-RTS

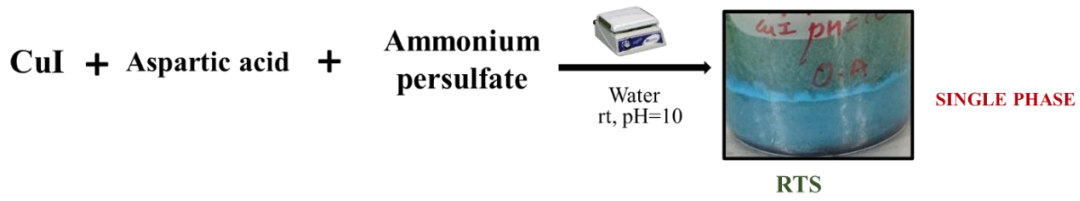

Scheme 4. *Schematic representation of synthetic procedure of AB-RTS*

Procedure:

To get single phase, homogeneous mixing of the solution is essential. Thus, we repeated the same procedure but this time under constant stirring. In brief, 50mM aspartic acid was added to 10mL of DI water. The pH of the solution was adjusted to 10 with the help of 1M NaOH solution. Then, under constant stirring of 600 rpm, 50 mM CuI was added followed by 100 mM APS. The resultant solution was stirred for 4 hours at 600 rpm and 45 ºC. At last, blue coloured precipitate was observed which was washed with

water and ethanol twice to remove any unreacted precursor. As we can see in **Scheme (4.)** only a single blue-coloured phase is observed.

After a few days of storage, it was observed the precipitate get evaporated. Therefore, to get the best possible results reaction optimization was done simply by varying different reaction conditions such as precursor metal salt, ratio of precursors, amount of oxidizing agent, *etc.* The procedure followed in each case are summarized hereafter-

3.6. Controlled Experiments

1. On changing metal salt:

Table 1. Controlled experiments performed by changing precursor metal salts.

Metal salt	**Amino acid**	**Oxidising agent**	**pH and Temp.**	**Solvent**	**Observation**
CuCl	L-Aspartic acid	APS	10 and rt	water	Initially some growth was there but later it get disappeared.
CuBr	L-Aspartic acid	APS	10 and rt	water	Initially some growth was there but later it get disappeared.

2. On changing the concentration of APS:

Table 2. Controlled experiments performed by changing concentration of APS.

Metal salt	**Amino acid**	**Oxidising agent**	**pH and Temp.**	**Solvent**	**Observation**
CuI	L-Aspartic acid	APS (10mM)	10 and rt	water	Blue coloured fibrous growth.
CuI	L-Aspartic acid	APS (25mM)	10 and rt	water	Two layers formed that is white and blue coloured layer.

CuI	L-Aspartic acid	APS (50mM)	APS (25mM)	water	Very thin white layer at bottom and scattered black layer.
CuI	L-Aspartic acid	APS (75mM)	APS (25mM)	water	Only black layer.

3. On changing the relative concentration of solvent:

Table 3. Controlled experiments performed by changing relative concentration of solvents.

Metal salt	**Ammino acid**	**Oxidising agent**	**pH and Temp.**	**Solvent**	**Observation**
CuI	L-Aspartic acid	APS	10 and rt	Methanol: water 1: 1	Only white layer was observed (very dark supernatant)
CuI	L-Aspartic acid	APS	10 and rt	DMSO: water 1: 4	Thin black glittery layer

4. On changing the oxidising agent:

Table 4. Controlled experiments performed by changing oxidising agents.

Metal salt	**Ammino acid**	**Oxidising agent**	**pH and Temp.**	**Solvent**	**Observation**
CuI	L-Aspartic acid	H_2O_2	10 and rt	water	Some precipitate was observed but not stable

5. On changing the relative concentration of L-Aspartic acid and metal salt:

Table 5. Controlled experiments performed on changing relative concentration of L-Aspartic acid and metal salt.

Precursor ratio	Oxidising agent	pH and Temp.	Solvent	Observation
CuI: L-Aspartic acid 1: 2	APS	10 and rt	water	Blue fibrous structure at bottom and above it some black rod like structure was observed
CuI: L-Aspartic acid 1: 3	APS	10 and rt	water	Blue fibrous structure at bottom and above it some white glittery layer was observed.

In all the abovementioned procedures, some growth was there. However, on storing them for longer period all the growth in the solution disappeared. Therefore, all these samples can't be used for further analysis.

3.7. Synthesis of CLA-16

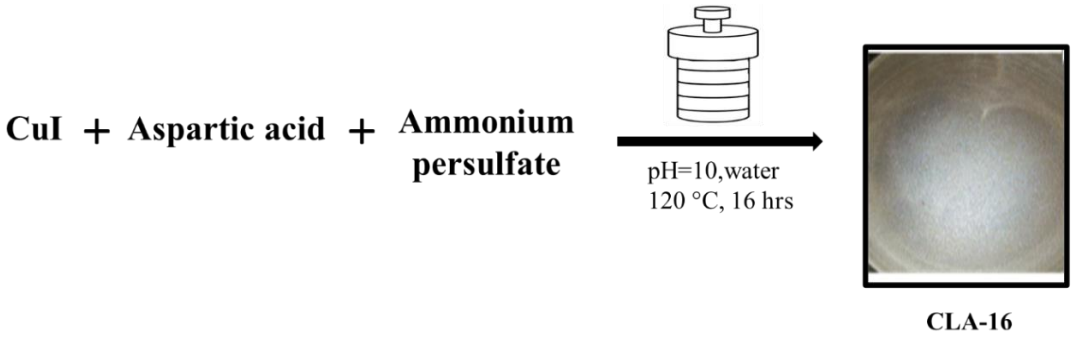

Scheme 5. *Schematic representation of synthetic procedure of CLA-16.*

To improve the stability of the sample, hydrothermal synthesis of the same solution was performed. The reaction procedure is similar to AB-RTS with an additional step. This step involves, the transfer of all the reaction mixture (with blue precipitate) into a 50 mL stainless steel lined Teflon autoclave. This autoclave is then kept in a preheated hot air oven for 16 hours at 120 ºC. After 16 hours, the solution was cooled naturally to

room temperature. The resultant solution consists of a shiny silverish precipitate along with a colorless supernatant which on UV irradiation showed blue fluorescence. The precipitate was then separated using centrifugation followed by washing with water and ethanol. The precipitate was finally collected after drying for further characterization.

Since this precipitate was stable at room temperature therefore to understand the mechanism in much better way, we performed some controlled experiments such as

(a) Role of APS: For this reaction, 50mM Aspartic acid was added to 10mL of DI water. The pH of the solution was adjusted to 10 with the help of 1M NaOH solution. Then, under constant stirring of 600 rpm, 50 mM CuI was added. The resultant solution was stirred for 1 hour at 600 rpm and 45 ºC. After this step, the reaction mixture (with greyish precipitate) was added into a 50 mL stainless steel lined Teflon autoclave. Autoclave was then kept in a preheated hot air oven for 16 hours at 120 ºC. After 16 hours, the solution was cooled naturally to room temperature. At last, grey coloured precipitate was observed which was washed with water and ethanol twice to remove unreacted precursor.

This observation hints that APS plays an important role in the formation of shiny, transparent CuI microcrystals.

(b) Role of aspartic acid: For this reaction, 50mM CuI was added to 10mL of DI water. The pH of the solution was adjusted to 10 with the help of 1M NaOH solution. Then, under constant stirring of 600 rpm, 100 mM ammonium persulfate was added. The resultant solution was stirred for 1 hour at 600 rpm and 45 ºC. After this step, the reaction mixture was added into a 50 mL stainless steel lined Teflon autoclave. This autoclave is then kept in a preheated hot air oven for 16 hours at 120 ºC. After 16 hours, the solution was cooled naturally to room temperature. At last, no precipitate was observed, only brown colored solution and some violet-coloured iodine crystals were having different morphologies were observed. (as we can see in figure). From this observation we can confirm that the presence of aspartic acid is crucial for the formation of microcrystals.

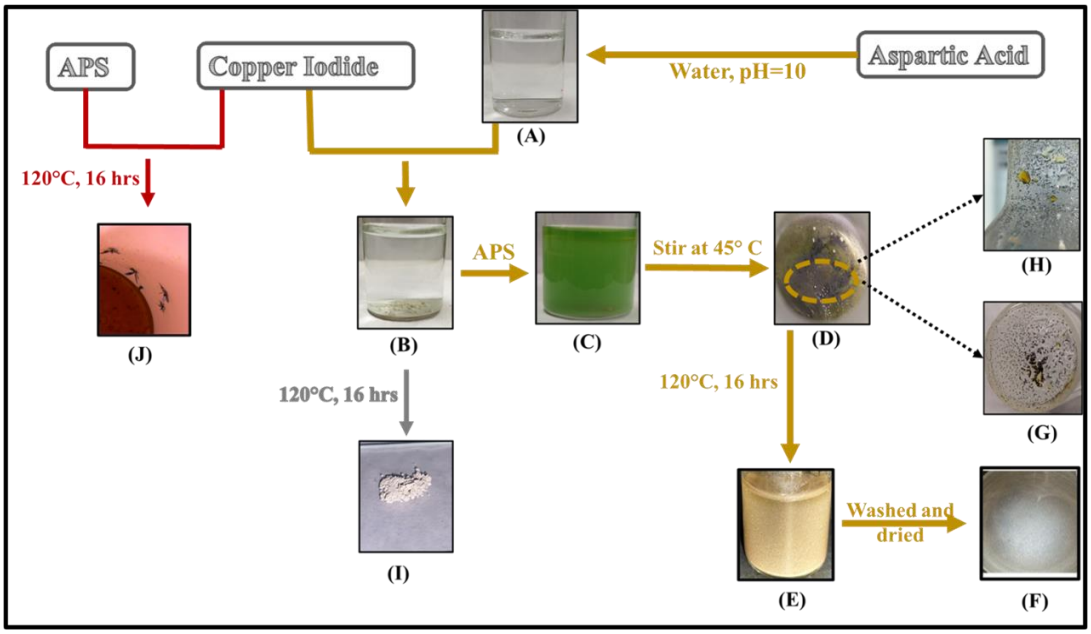

Figure 7. (A-F) *Schematic representation of optimized synthetic procedure for CLA-16. Digital images of* ***(A)*** *transparent solution of AA* ***(B)*** *precipitate formed after adding CuI.* ***(C)*** *green colored solution* ***(D)*** *formation of iodine crystals (magnified image showing deposited crystals on* ***(H)*** *RB flask* ***(G)*** *lid.* ***(E)*** *Shiny microcrystal of CLA-16.* ***(F)*** *CLA-16 after washing and drying.* ***(I)*** *Amorphous powder of CL-16.* ***(J)*** *Insect like Iodine crystals deposited on autoclave in Teflon.*

3.8. Interaction of Cu(I) with other amino acids

In nature, 20 amino acids are present. These amino acids differ in their structure which tune their properties. Therefore, amino acids having different properties (acidic, basic, and neutral), structure (aromatic and aliphatic) were employed while keeping all the other reaction conditions intact. The table below summarizes different reaction conditions used in each case.

Table 6. Controlled experiments performed on changing organic ligands

Metal salt	**Organic ligand**	**Oxidising agent**	**Solvent**	**pH, Temp. and Time**	**Observation**
CuI	Glutamic acid	APS	water	10, 120 ºC and 16 hrs.	Crystalline brown coloured
CuI	Histidine	APS	water	-, 120 ºC and 16 hrs.	amorphous Black coloured
CuI	Tryptophan	APS	water	10, 120 ºC and 16 hrs.	Crystalline brick red coloured
CuI	Glycine	APS	water	10, 120 ºC and 16 hrs.	Crystalline brown coloured
CuI	Citric acid	APS	water	10, 120 ºC and 16 hrs.	Crystalline brown coloured
CuI	Ascorbic acid	APS	water	10, 120 ºC and 16 hrs.	Crystalline brown coloured

Chapter 4

Result and discussion

After carefully optimizing all the reaction conditions, a highly stable crystalline product was formed in the case of CLA-16. This product was then characterized via various techniques to get insight into its clear morphological and chemical composition.

4.1. FESEM and EDX spectra

The morphology, size, and distribution of elements throughout the CLA-16 were studied by microscopically (FESEM) and spectroscopically (EDS), and the formation of three-dimensional hexagonal crystal structure was observed in the case of CLA- 16 of length 7.2mm and breadth 5.2 mm as shown in the **(Figure 8. B).** Moreover, EDX depicts that the synthesized CLA-16 is composed of elements like C, O, Cu, and I with atomic % of 35.97, 7.94, 31.77 and 24.33 respectively (**Table 7.** and **Figure 9. F**). Moreover, elemental mapping clearly shows the uniform distribution of C, O, and Cu and I throughout the morphology of CLA-16 **(Figure 9. B, C, D and E).** For other cases of controlled experiments also FE-SEM and POM images were recorded which are given in Figure(c) & figure (d) in supporting information respectively.

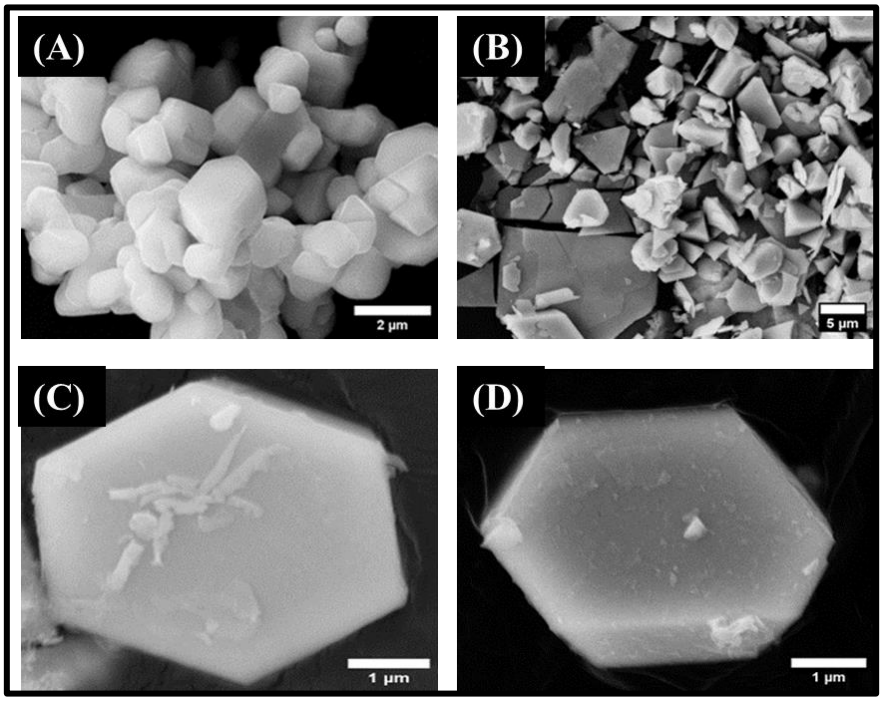

Figure 8. *FE-SEM images of (A) CL-16 (B) CLA-4 (C) CLA-16 (D) CLA-72.*

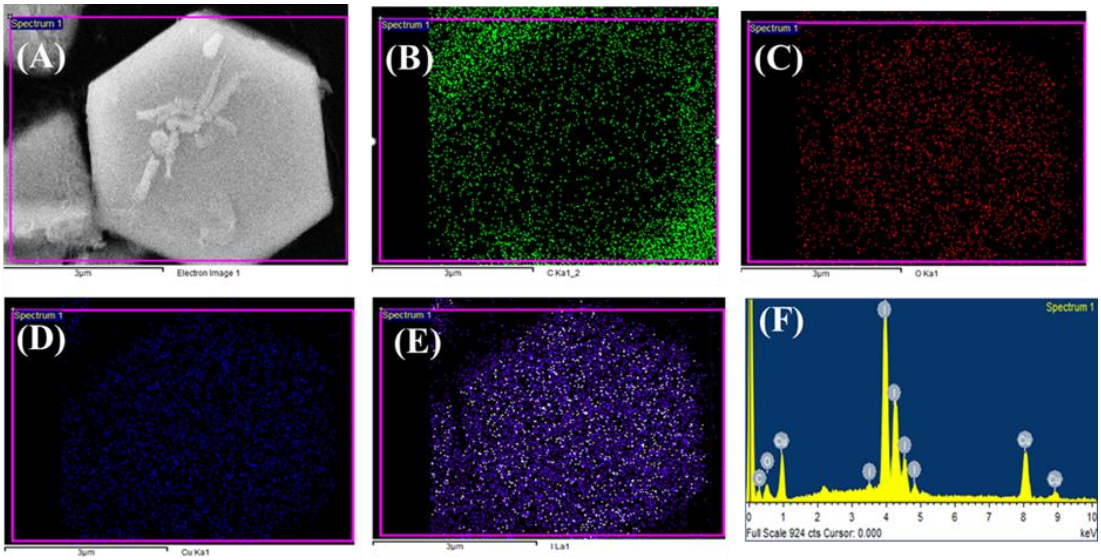

Figure 9. ***(A)*** *FE-SEM images of CLA-16* ***(B-E)*** *EDX elemental mapping images of CLA-16 and* ***(F)*** *EDX spectrum of CLA-16.*

Table 7. Percentage composition of elements in CLA-16

Element	**C**	**O**	**Cu**	**I**
Atomic %	68.42	9.41	11.04	11.13
Weight %	26.63	4.88	22.73	45.77

4.2. FTIR spectroscopy

The interaction between Cu(I) and L-Aspartic acid at pH 10, when an oxidizing agent *i.e.* APS was used, further portrayed by comparing the FTIR spectra of L-Aspartic acid and CLA-16 (**Figure 10**). In the FTIR spectrum of L-AA, the peak centred at 1685 cm^{-1} can be assigned to CO stretching of the carboxylic group, and the peaks at 1501 cm^{-1} and 1419 cm^{-1} were credited to COOH stretching vibrations. The peaks positioned at 1640 cm^{-1} and 1597 cm^{-1} were assigned to NH stretching and bending.[13] The peak at 1149 cm^{-1} resembles to NH_2 rocking mode. In the case of CLA-16, the peak at 1685 cm^{-1} is shifted to 1719 cm^{-1}, the peak at 1501 cm^{-1} has vanished, and the peak at 1419 cm^{-1} is shifted to 1444 cm^{-1} which confirms that the carboxylic group of LAA is interacting with metal centre. The peak at 1597 cm^{-1} is shifted to 1594 cm^{-1} with reduced intensity while the peak at 1149 cm^{-1} is shifted to 1167 cm^{-1} which signifies amine group interaction with metal ion. Shifting is due to the change in the electronic environment

in the molecules after interacting with copper ion. Shift in the peaks of FTIR was also observed in the case of RT which is given in Supporting Information.

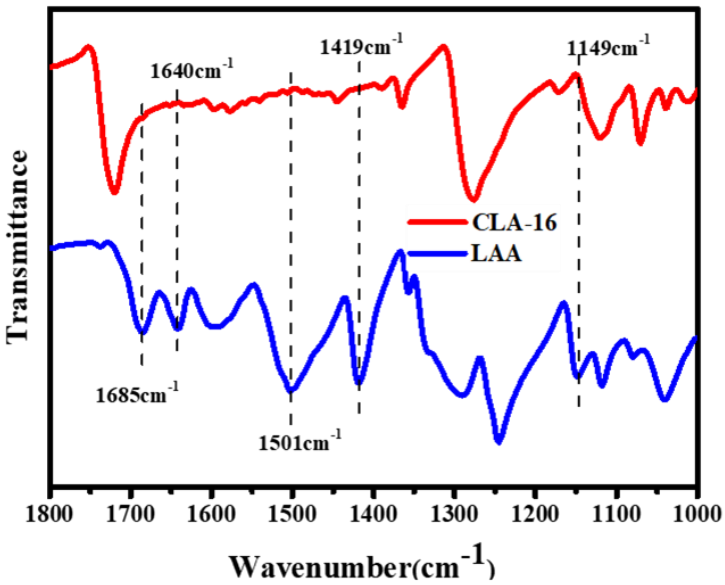

Figure 10. *FTIR spectra of L-Aspartic acid and CLA-16.*

4.3. Powder X-ray Diffraction (PXRD)

Powder XRD is a useful technique which gives us insight about the crystallinity of the sample, crystal structure, interplanar distance *etc.* Therefore, PXRD of CLA-16 was recorded. Sharp peaks in the XRD pattern of a sample show high crystallinity of the synthesized samples. After carefully comparing pattern with available data of CuI in literature it was observed that the growth is preferentially in (111) direction. The peak in CLA-16 at 25.38°, 29.42°, 42.1°, 49.84°, 52.12°, 61.12°, 67.32°, 69.26° and, 77.04° resembles with plane (111), (200), (220), (311), (222), (400), (331), (420) and, (422) respectively. The peaks in CLA-72 and CL-16 also matches precisely with the CuI.[24]

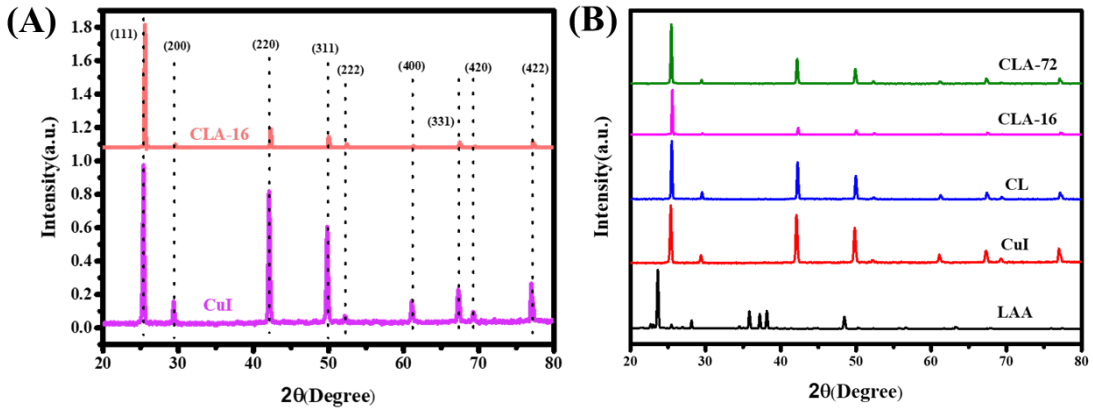

Figure 11. *(A) PXRD pattern of CuI and CLA-16.* ***(B)*** *PXRD pattern of LAA, CuI, CL, CLA-16 and CLA-72.*

4.4. Thermogravimetric Analysis (TGA) and Differential thermal Analysis (DTA)

TGA is used to check the thermal stability, purity and composition of the material and thermal stability of the compound at which any further experiment could be done. After analyzing the TGA data (**Figure 12**), the increase in weight is due to the adsorption of N_2 gas. After 425ºC, rapid decomposition of material could be confirmed by weight loss of approx. 60 percent. DTA curve which is derived from TGA shows a sharp peak near 600ºC which signifies the decomposition of crystal which is an endothermic process BioMOF RT was stable up to 200ºC as given in Supporting Information in Figure (b).

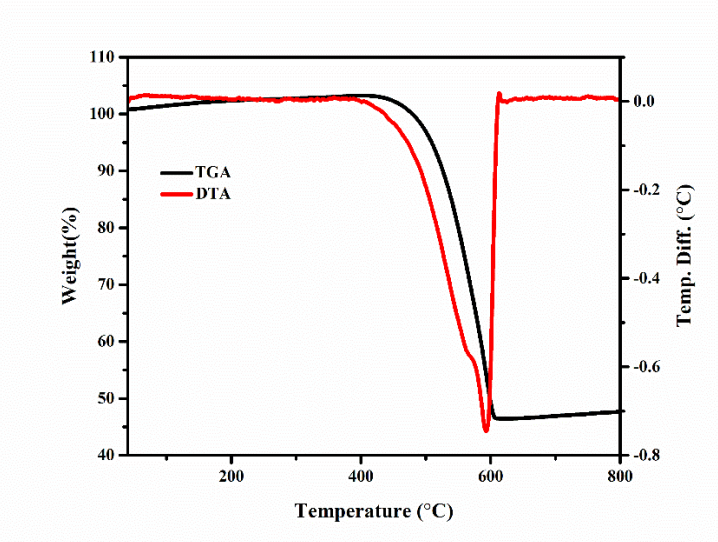

Figure 12. *TGA and DTA curve of CLA-16 in N_2 environment.*

4.5. Brunauer-Emmett-Teller (BET)

the surface area and pore size measurement of the catalyst is of utmost requirement as catalytic efficiency is directly related to the surface area and pore size of the catalyst. So, the surface area and porosity of CLA-16 was measured by N_2 adsorption-desorption experiment at 77 K (**Figure 13 A**). Moderate N_2 gas uptaking capacity was attributed to the moderate surface area of 42.878 m^2g^{-1} as calculated by BET model. BJH (Barret–Joyner–Halenda) method was used to calculate the pore volume and average pore diameter ofCLA-16, and the values were found to be .067 cc/g and 4.942 nm respectively **(Figure 13 B).**

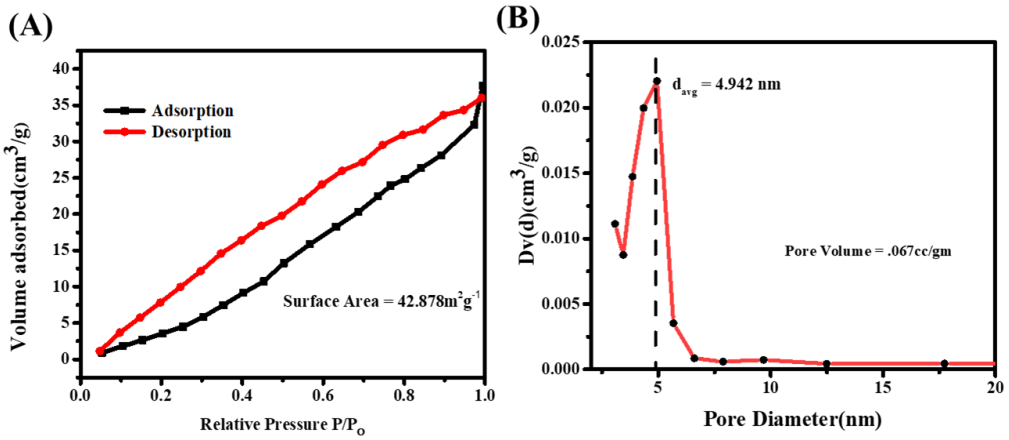

Figure 13. (A) *Nitrogen adsorption isotherm for CLA-16 recorded at 77 K to measure the surface area.* ***(B)*** *Average pore size distribution of CLA-16.*

4.6. X-ray photoelectron spectroscopy (XPS)

Further analysis of the elemental composition over the surface of CLA-16 and the oxidation state of Cu was examined using XPS. The wide range XPS survey spectrum specifies the presence of C, O, N, I and Cu which is consistent with the result obtained from the EDX **(Figure 9)**. Moreover, in the high resolution XPS spectrum of Cu 2p **(Figure 14 F)**, the characteristic peaks located at the binding energies of ~932 eV and ~951.8 eV corresponds to the Cu $2p_{3/2}$ and Cu $2p_{1/2}$, respectively. The spin-orbital splitting (Cu $2p_{3/2}$ - Cu $2p_{1/2}$) value, which is 19.8 eV obtained from the Cu 2p spectrum indicates that copper is in +1 oxidation state. Iodine $3d_{5/2}$ and $3d_{3/2}$ peaks appear at BE values of 619 and 630.5 eV, respectively, as shown in the spectrum **(Figure 14 E)**. These binding energy values are also consistent with previously reported values. In O 1s spectrum **(Figure 14 B)** there is one peak at 531.8 eV correspond to the C=O group of COOH moiety of Aspartic acid. The deconvoluted C 1s spectrum shows four peaks

(Figure 14 C). The C-NH_3^+ interaction in the Aspartic acid was related with the binding energy value of 284.5 eV. The peak at 286 eV resembles to the C-COO^- group of aspartic acid. The peak at 288.4 eV matches to the C=O group of Aspartic acid and there is a very diminished peak at binding energy of 289.4 eV which resembles with -COOH group of Aspartic acid. Additionally, the deconvoluted N 1s spectrum presents two peaks **(Figure 14 D).** The peak at 400.4 eV (more intense) corresponds to the NH_2 group of Aspartic acid. The peak at 405.1 eV (less intense) corresponds to the oxidised nitrogen peak. From this oxidised nitrogen peak we can say that aspartic acid is reducing the copper from +2 to +1 oxidation state. (Because in our synthetic procedure we have used ammonium persulfate to oxidise Cu. Therefore, XPS spectra confirms that Cu is in +1 oxidation state and aspartic acid is reducing the Cu. In CLA system copper is in +1 oxidation state.[25]

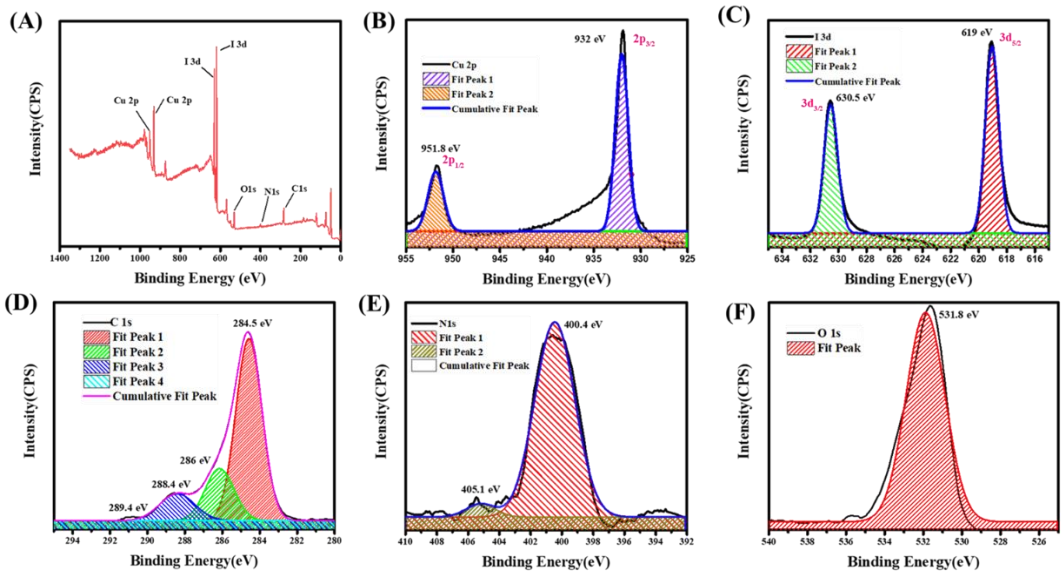

Figure 14. (A) *Wide angle XPS spectrum of CLA-16; High resolution XPS spectra of* ***(B)*** *O 1s* ***(C)*** *C 1s* ***(D)*** *N 1s* ***(E)*** *I 3d* ***(F)*** *Cu 2p.*

4.7. UV-Visible spectroscopy

UV-Visible spectra were recorded for CLA-16 solutions in acetonitrile, which then compared with spectra of CuI and CL-16 solution in same solvent. The two peaks of high intensity (near 207 nm and 245 nm) are present in all the three samples. However, in the case of CLA-16, small hump was observed starting from 300 nm. To get absorption peak of significant intensity, concentration-dependent spectra was recorded which at higher concentration showed a clear absorption band centred at 360 nm. The

band gap was calculated with the help of Tauc's formula using the absorbance data. Which showed intercept at 3.03eV. Generally, the band gap of CuI thin films lies between 2.7 to 3.14 eV.[9]

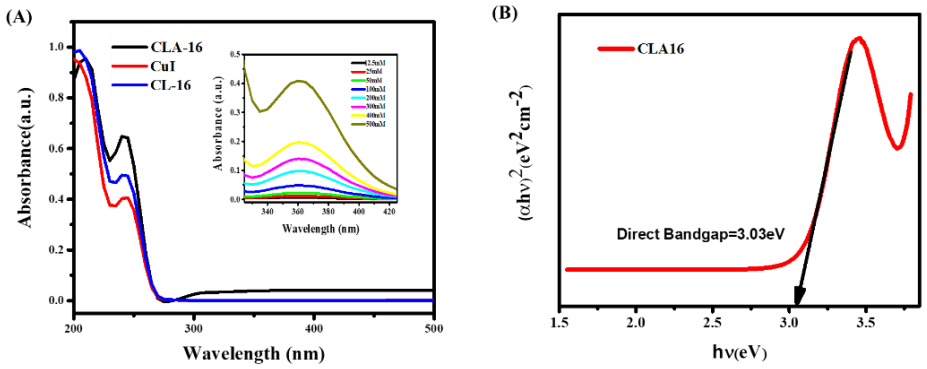

Figure 15. ***(A)*** *UV-vis Spectra of CLA-16, CuI and CL-16. (Inset: UV-vis spectrum showing the evolution of peak at 360 nm by increasing the concentration of solution)* ***(B)*** *Tauc's plot.*

4.8. Circular Dichroism (CD) Spectroscopy

Circular dichroism (CD) is a spectroscopic method that measures the change in the absorption of left-handed and right-handed circularly polarized light by chiral molecules. CD spectra were measured for both L-aspartic acid and CLA-16. L-aspartic acid displayed a sharp peak at 203 nm, while CLA-16 showed a reduction or loss of this peak, which confirms negligible amount of amino acid is present.

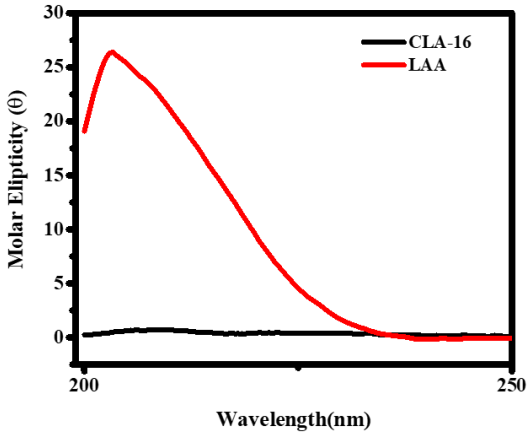

Figure 16. *CD-Spectra of LAA and CLA-16.*

4.9. Enzyme mimicking activity

4.9.1. Oxidase-like activity

Oxidase activity refers to the capability of a substance or enzyme to facilitate oxidation reactions by promoting the transfer of electrons from a substrate to an oxygen molecule or another electron acceptor.

To determine the oxidase-like activity of CLA-16, 3,3'5,5'-tetramethylbenzidine (TMB) was used as a chromogenic substrate. TMB is colourless in its original form. To check the oxidase activity, we form two following sets.

Set-1. 900 µL Acetate Buffer (0.1M) @pH 4 + 100 µL TMB (1mM).

Set-2. 900 µL Acetate Buffer (0.1M) @pH 4 + 100 µL TMB(1mM) +Catalyst (0.33mg/ml).

The absence of any observable color change, even over an extended period, suggests that the catalyst did not exhibit oxidase activity during the preliminary test.

4.9.2. Haloperoxidase-like activity

Haloperoxidase activity refers to the catalytic capability of enzymes to facilitate reactions involving halides (such as chloride, bromide, or iodide) in the presence of H_2O_2. These enzymes can oxidize halides to form hypohalous acids or their derivatives. Since in our system iodide metal salt was present, we also tried the preliminary test to check the catalytic activity of our system at different pH, but no color change was observed.

4.9.3. Peroxidase-like activity

Peroxidases are enzymes that play a vital role in catalyzing redox reactions in organisms.[26] They are known for their ability to utilize hydrogen peroxide to oxidize a wide range of substrates.

To determine the peroxidase-like activity of CLA-16, 3,3'5,5'-tetramethylbenzidine (TMB) was used as a chromogenic substrate. TMB is colorless in its original form. To check the peroxidase activity, we form two following sets.

Set-1. 870 µL Acetate Buffer (0.1M) @pH 4 +30 µL H_2O_2 (5mM) + 100 µL TMB (1mM).

Set-2. 870 µL Acetate Buffer (0.1M) @pH 4 +30 µL H_2O_2 (5mM) + 100 µL TMB(1mM) +Catalyst (0.33mg/ml).

To initially test the peroxidase-like activity of CLA-16, two samples were prepared as previously described. The color change of the solution was observed. The color of the microcentrifuge tube containing the catalyst turned blue within 15 minutes **(Figure 17)** and deepened over time. This change confirms the peroxidase-mimicking activity of CLA-16.

Figure 17. *Images showing the oxidation of TMB at the different time confirming the peroxidase-like activity of CLA-16.*

TMB was chosen as the chromogenic substrate to assess the peroxidase-like activity of CLA-16. When TMB was mixed with hydrogen peroxide, the solution turned a pale blue. However, the addition of CLA-16 accelerated the chromogenic reaction, darkening the solution. The blue product in both reactions was oxTMB, which exhibited a characteristic absorption peak at 625 nm. UV-vis spectra confirmed that TMB could not be oxidized without hydrogen peroxide, and the catalyst was inactive without hydrogen peroxide. These findings demonstrate that all three components—TMB, H_2O_2, and the catalyst—are required to oxidize the substrate, confirming the peroxidase-like behavior of CLA-16 at acidic pH. Oxidation of TMB was monitored in the presence of the catalyst, UV spectra were recorded in every 5 minutes up to 60 minutes to get a quantitative understanding of the rate at which the reaction is proceeding. It has been observed that the peak intensity increases constantly confirming more amount of TMB getting oxidized. **(Figure 18)**

Environmental factors significantly influence the efficiency of enzyme catalysis, and similar effects are expected for peroxidase-mimicking materials like CLA-16. A series of experiments were conducted to assess how various conditions, such as pH, reaction temperature, concentrations of TMB and H_2O_2, and reaction time, affect the peroxidase-like activity of CLA-16.

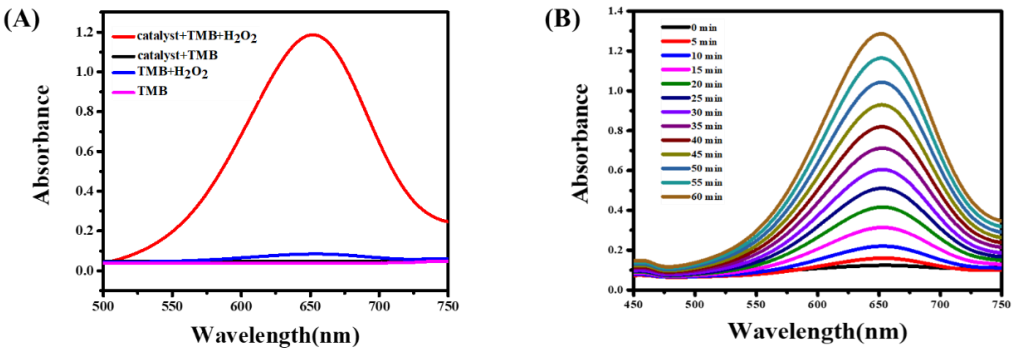

Figure 18. (A) *UV-Vis spectra showing the oxidation of TMB in various conditions: i) in presence of H_2O_2 and CLA-16, (ii) in presence of CLA-16, (iii) in presence of H_2O_2, and (iv) Only TMB.* ***(B)*** *Time-dependent monitoring of CLA-16 (1mg/ml)-catalyzed oxidation of TMB(1mM) for 1 hour using UV-visible spectrophotometer.*

Since acidic amino acids are reported to exhibit intrinsic peroxidase activity, different controls with all the precursors were performed. Kinetics studies were conducted for aspartic acid, CuI, a combination of CuI and aspartic acid at high temperature (CL-16), and CLA-16 using chromogenic substrate TMB (100 µL, 1Mm) in presence of hydrogen peroxide (30 µL, 5mM) in acetate buffer (870 µL, 100 mM). The **(Figure 19)** clearly demonstrates that CLA-16 exhibits the highest catalytic activity among the tested samples.

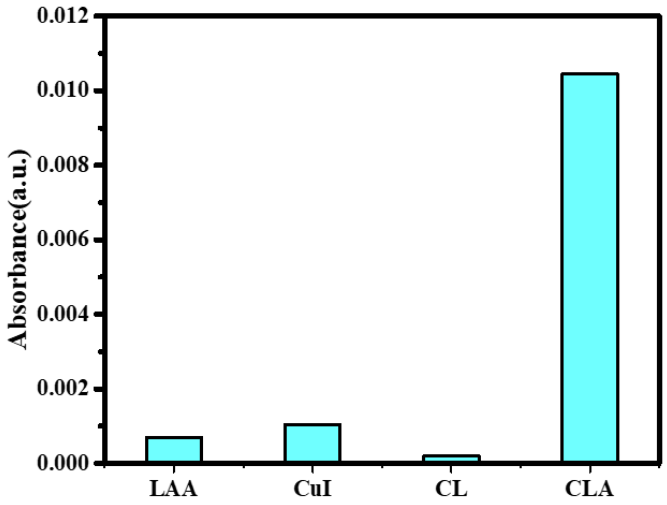

Figure 19. *Bar graph of time dependent kinetic analysis of LAA, CuI, CL-16 and CLA-16.*

The pH of the reaction mixture can impact the ionization state and reactivity of the components, as well as the stability of the catalyst. Optimizing the pH ensures maximum peroxidase-like activity of CLA-16.

To investigate the effect of pH on CLA-16's activity, the oxidation of TMB (1 mM) was tested in the presence of 5 mM H_2O_2 and 0.33 mg/mL of the catalyst in acetate buffer; for alkaline conditions, phosphate buffer was used. By observing the results (as shown in the figure), we can conclude that the maximum oxidation of TMB occurs at pH 4, indicating that CLA-16's catalytic activity is highest at this pH.

For enzyme mimics, it's crucial that they maintain their activity across a broad range of pH levels. To further examine the performance of CLA-16 at different pH values, the catalyst was immersed in buffers with pH 2, 7, and 10 for three days. After this period, the catalyst was removed from the buffer, washed, and dried. The figure shows that the PXRD data of the catalyst, following incubation at various pH levels, closely matches the PXRD data of CLA-16, indicating that its structure is preserved across the wide range pH.

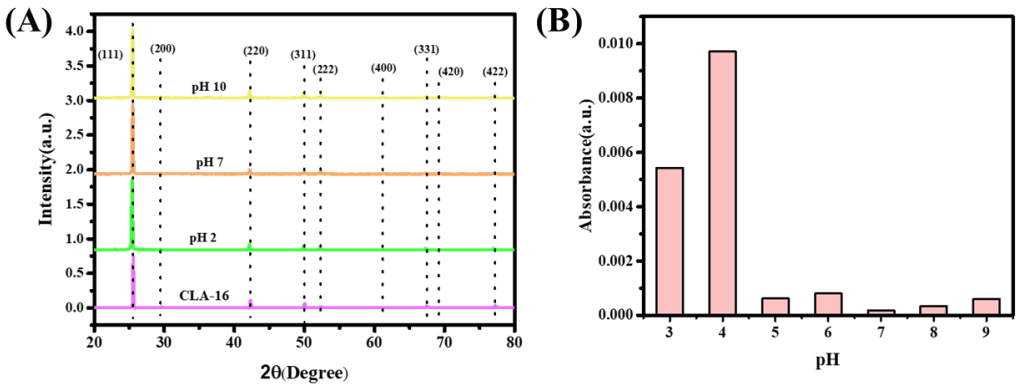

Figure 20. *(A) Comparison of PXRD of immersed catalyst at different pH for 3 days.* ***(B)*** *Bar graph showing effect of pH on the peroxidase-mimic activity of CLA-16.*

Elevated temperatures typically cause the denaturation of native enzymes, resulting in a complete loss of activity and limiting their practical applications. To verify this, we assessed the enzymatic activity of CLA-16 at high temperatures. CLA-16's catalytic activity was assessed after incubation at various temperatures ranging from 20°C to 80°C. The figure shows that the catalytic activity of CLA-16 increases with rising temperature. Even at very high temperatures, the catalyst continues to maintain its activity.

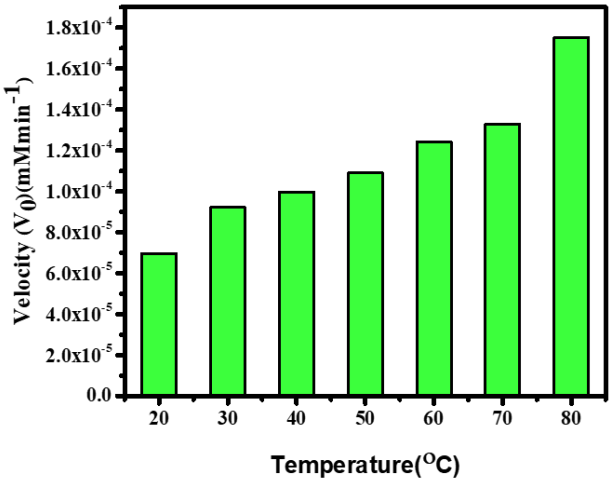

Figure 21*. Bar graph showing effect of temperature on peroxidase-mimicking activity of CLA-16.*

In the case of HRP, enzyme activity significantly decreases after exposure to pH levels below 5 or temperatures above 40°C for just 2 hours. In contrast, CLA-16 maintains its activity across a broad range of pH levels and temperatures. Varying the concentrations

of TMB and hydrogen peroxide allows for the evaluation of the reaction's sensitivity to substrate availability. A certain ratio between TMB and H_2O_2 may yield optimal activity.

To gain understanding of the mechanism of CLA-16's peroxidase-like activity, steady-state kinetics experiments were conducted. It's well established that the oxidation of TMB using natural peroxidases such as horseradish peroxidase (HRP) depends on the concentrations of both TMB and H_2O_2. Therefore, the concentration of one substrate (TMB or H_2O_2) was varied while keeping the other substrate concentration and the catalyst constant.

The peroxidase-mimicking activity of CLA-16 was evaluated by measuring the initial reaction rate (V_0) at varying TMB concentrations (0.1 mM to 8 mM), while keeping H_2O_2 (5 mM) and the catalyst (0.33 mg/mL) constant. A linear increase in V_0 was observed at lower TMB concentrations, but as TMB concentration increased, the rate of change diminished, indicating concentration-dependent saturation of the rate, which aligns with the Michaelis-Menten model (Figure). Similar to TMB, varying H_2O_2 concentrations (0.5mM to 5.5 mM) keeping TMB (1 mM) and the catalyst (0.33 mg/mL) constant shows the Michaelis-Menten type of kinetics.

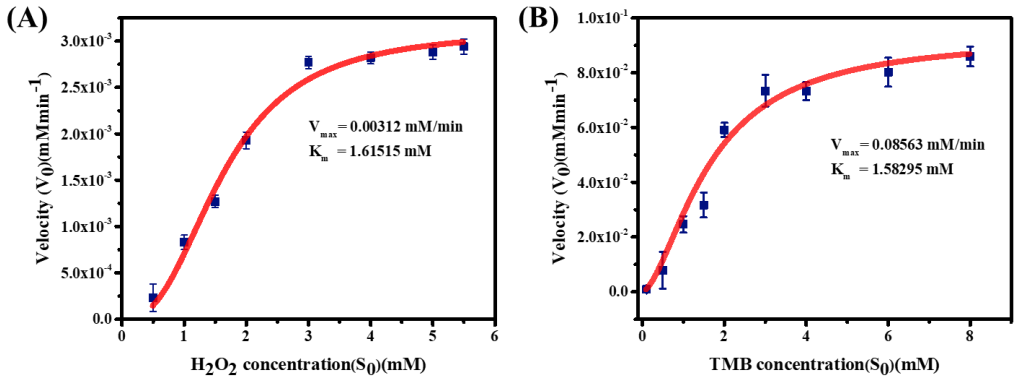

Figure 22. (A) *Steady state kinetics assay, velocity of the reaction measured using 0.33 mg/ml CLA-16 with respect to the concentration of H_2O_2 and* ***(B)*** *Steady state kinetics assay, velocity of the reaction measured using 0.33 mg/ml CLA-16 with respect to the concentration of TMB.*

The Michaelis-Menten equation describes the relationship between the rate of substrate conversion by an enzyme and substrate concentration. V_0 is the initial reaction rate, Vmax is the maximum rate of conversion, [S_0] is the substrate concentration, and K_m is

the Michaelis constant, representing the substrate concentration at which the conversion rate is half of V_{max}, indicating the enzyme's affinity for the substrate.

$$\frac{1}{V_0} = \frac{K_m}{V_m} \times \frac{1}{S_0} + \frac{1}{V_{max}}$$

Table 8. Comparison of the Michaelis–Menten constant (K_m) of different peroxidase mimicking materials

Catalyst	Substance	K_m(mM)	Reference
Aspartic acid	TMB	0.4370	27
	H_2O_2	0.0115	
HRP	TMB	0.1790	[27]
	H_2O_2	1.180	
Cu-hemin MOF	TMB	1.42	[28]
	H_2O_2	2.18	
Cu-MOF	TMB	2.4862	[29]
	H_2O_2	0.163	
CuS	TMB	0.0072	[30]
	H_2O_2	12.0	
CuO NPs	TMB	0.013	[31]
	H_2O_2	85.6	
Hemin@MIL-101	TMB	0.068	[32]
	H_2O_2	10.9	

The kinetic parameters, that is V_{max} and K_m of CLA-16 with H_2O_2 were found to be

0.00312 mM/min and 1.61515 mM respectively and for TMB values of V_{max} and K_m are 0.08563mM/min and 1.58295mM respectively. The K_m value of CLA-16 for TMB and H_2O_2 are much lower than the K_m value of natural HRP which shows the good affinity of CLA-16 with substrate than HRP. Then K_m value was compared with other reported peroxidase mimicking materials **(Table 8)**, the lower K_m value for our catalyst suggests the higher affinity for substrate.

Mechanism:

In natural peroxidase enzymes, usually two different mechanisms are known. The reaction can proceed through electron transfer or •OH formation. To evaluate which mechanistic pathway is being followed in present case, terephthalic acid was employed as a fluorogenic marker in the reaction medium. Terephthalic acid interact with •OH to form 2-hydroxyterephthalic acid that emits in the blue region. The generation of hydroxyl radicals was assessed by dispersing CLA-16 (0.33mg/ml) in 3.0 mL of sodium acetate buffer (pH 4.0) containing 5 mM H_2O_2, 1mM TMB, and 0.33mM Terephthalic acid. **(Figure 23A)** shows in the presence of catalyst intensity of the peak centred at 410 nm increased significantly with time. This result confirms that the reaction proceeds through OH radical formation. Control experiments indicate that only CuI and L-AA separately have poor activity when compared with CLA-16. This result hints towards synergistic effect of both CuI and L-AA. In past, high affinity of acidic amino acids (due to COOH groups) towards H_2O_2 was found to be responsible for their peroxidase-mimic behaviour. Various spectroscopic techniques confirmed the presence of aspartic acid in CLA-16. IR data of CLA-16 indicate the capping is preferentially through NH_2 leaving COOH groups free to form H-bonds with H_2O_2. Due to H-bonding, OH radicals are formed facilely. Copper-based various peroxidase-mimics are known in the literature. In general mechanism, first step include first conversion of Cu(II) to Cu(I) which then further react with H_2O_2 to produce •OH which is then responsible for the oxidation of TMB. In present case, the catalyst is already present in +1 oxidation state, which simply reduces one step making the reaction process faster. Based on the abovementioned observations, a plausible mechanism can be proposed where capped L-AA binds with H_2O_2 while Cu binds with TMB which brings both the substrates in a close proximity, therefore facilitating the reaction. The synergistic effect of both results in enhanced radical generation which enhances the rate of oxidation

manifolds. The Cu(II) then can be reduced back to Cu(I) with H_2O_2 regenerating the active site of the catalyst.

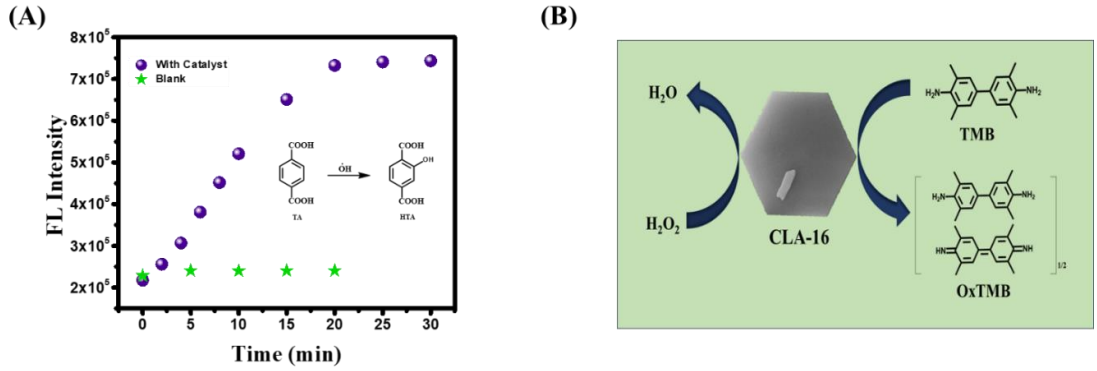

Figure 23. (A) *Increase in fluorescence intensity with time using Terephthalic acid (TA) as a fluorescent probe in the presence of CLA-16. (B) Schematic representation of the peroxidase-like activity of CLA-16 using TMB as substrate in presence of* H_2O_2.

4.10. Other potential applications

4.10.1. Fluorescence

CuI based materials are well known to show luminescence (fluorescence and phosphorescence) in visible region.[33] Due to emissive nature of these materials, they are widely used as fluorescent inks. Therefore, we explored emissive nature of CLA-16 using fluorescence spectroscopy and microscopy. As initial observation, upon irradiation with UV light (λ=365 nm) orange fluorescence was observed. To get quantitative proof, solid state fluorescence spectra for the dropcasted sample was recorded which showed broad emission with peaks centred in blue (λ=425 nm and 457 nm), green (λ = 517 nm), and red region (λ = 683 nm) of the visible spectrum. (Figure). In solution state, CLA-16 (in acetonitrile) shows emission at 400nm and 425 nm when excited at 365 nm (Figure)

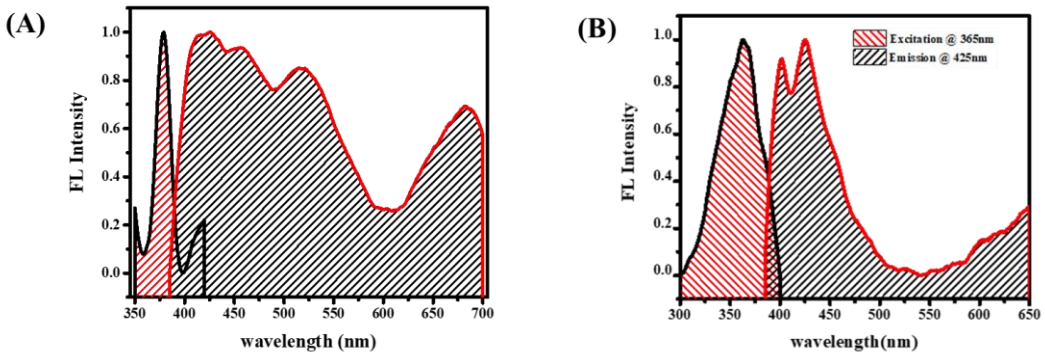

Figure 24. (A) *Fluorescence spectra of CLA-16 (solid form)* ***(B)*** *Fluorescence spectra of CLA-16 in solution (acetonitrile).*

4.10.2. Solvatochromism

Various CuI based materials such as MOFs, nanoclusters, nanoparticles show change in their emission maxima on changing the solvent (phenomenon known as solvatochromism).[34] This behaviour is important for sensing application. CLA-16 when dissolved/dispersed in different solvents, it showed emission at different wavelengths.

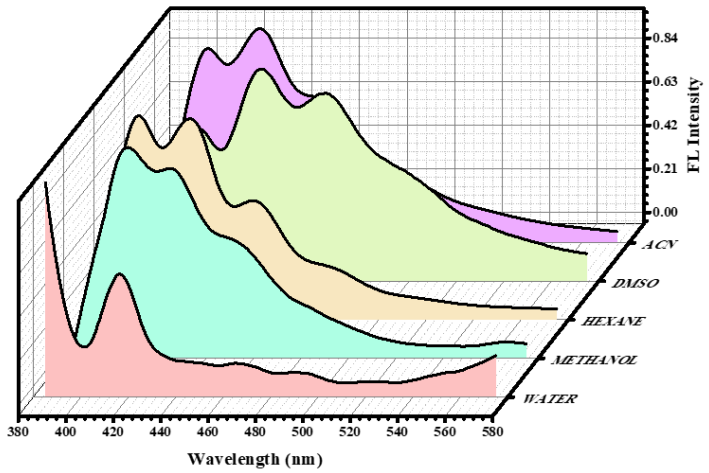

Figure 25. *3D waterfall graph showing shift in emission spectra of CLA-16 when dispersed/dissolved in different solvents on exciting at λ=365nm.*

4.11 Interaction of Cu(I) with other amino acids

4.11.1 Thermogravimetric Analysis (TGA)

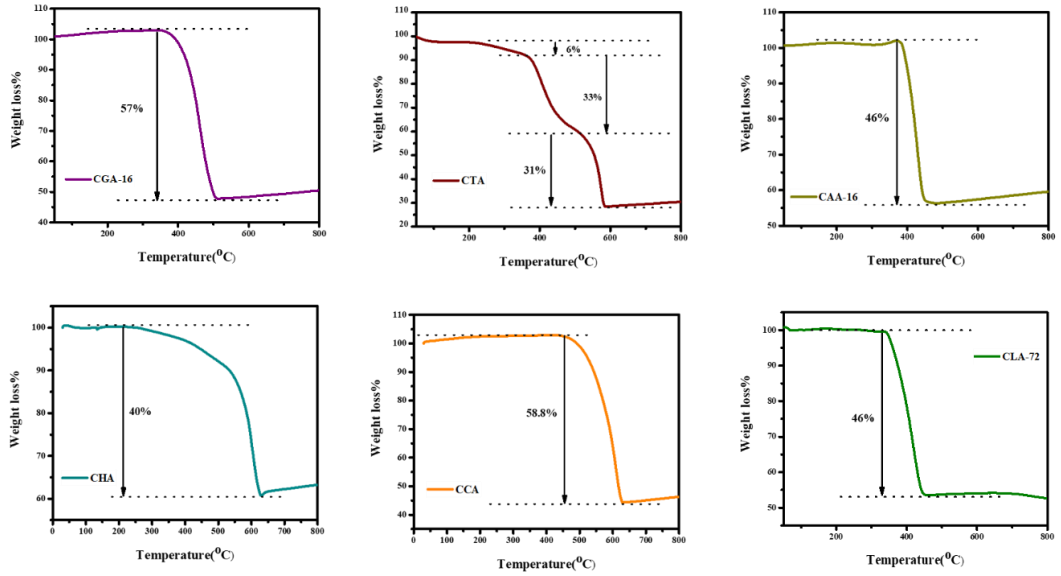

Figure 26. *TGA curves of CGA-16, CTA-16, CAA-16, CHA-16, CCA-16, and CLA-72 in N_2 environment.*

Thermal stability of all the synthesized sample was measured through TGA analysis that showed similar pattern like CLA-16. Different behavior was observed when aromatic amino acids were used as capping agent.

4.11.2 Powder X-ray Diffraction (PXRD)

To check the effect of different type of amino acids/biomolecules on the directional growth of CuI microcrystals, PXRD was recorded. It was observed that in every case CuI is formed as all the characteristic peaks are present. On the contrary, relative intensities of these peaks varies significantly on changing capping agents. Exceptionally in the case of CHA-16 broad peaks indicate amorphous nature of sample.

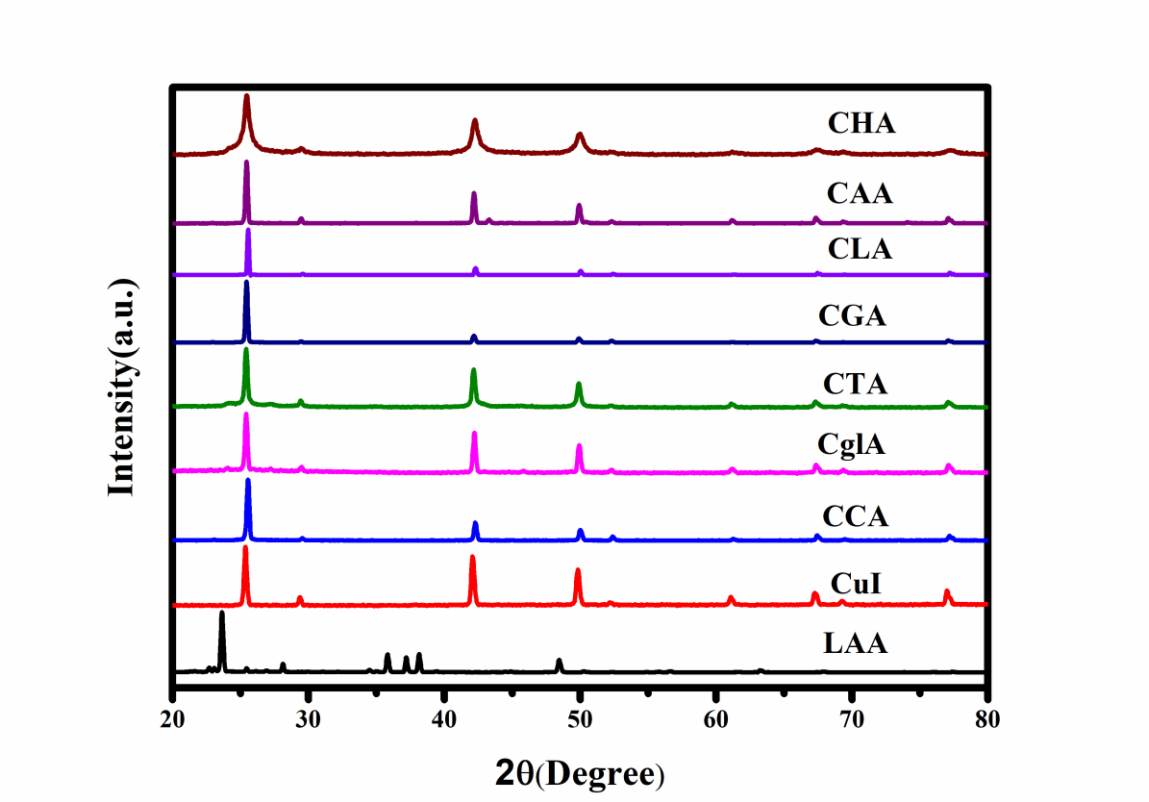

Figure 27. *PXRD data of LAA, CuI, CCA-16, CglA-16, CTA-16, CGA-16, CLA-16, CAA-16, CHA-16 in N_2 environment.*

4.11.3 FESEM

The effect of using different amino acid as capping agent was monitored using FESEM instrument. In each case different type of morphologies were observed such as in the case of CTA-16, spherical ball like morphology was observed. In CCA-16, sheet like structure were present. In CGA-16, hexagon shaped morphology was observed which is similar to CLA-16. Beautiful flower-like structures were present in CHA-16. 3D Rods were observed in CglA-16. In CAlA-16, multiple hexagons fused together making a sheet like appearance when observed.

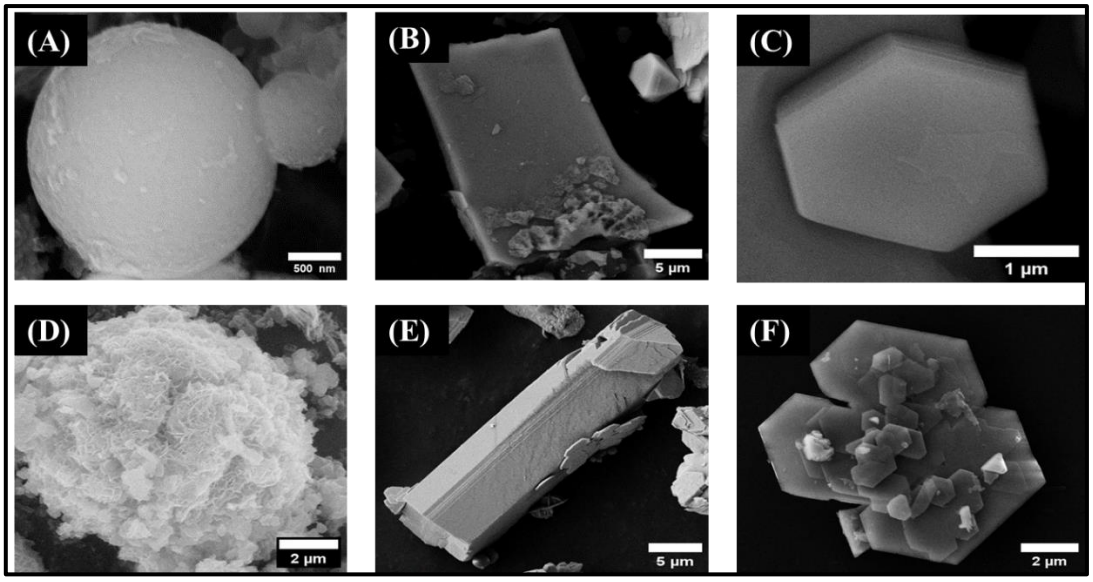

Figure 28. *FE-SEM images of* ***(A)*** *CTA-16* ***(B)*** *CCA-4* ***(C)*** *CGA-16* ***(D)*** *CHA-16 and* ***(E)*** *CglyA-16.* ***(F)*** *CAlA-16.*

Chapter 5

Conclusion

In the present work, various attempts were made to develop a MBioFs using Cu(I) salts and an acidic amino acid (aspartic acid). Initially, due to weak solubility of CuI in water, no satisfactory results were observed. Thus, a mild oxidizing agent was introduced in the reaction that leads to formation of three different phases which were not stable when separated. After optimizing reaction conditions, hydrothermal treatment of the reaction medium resulted in the formation of stable shiny and crystalline precipitate. Various spectroscopic techniques such as FTIR, XPS, EDS *etc.* confirms presence and interaction of AA with metal ions. FESEM images show hexagonal microcrystals of CLA-16. In contrast, PXRD pattern precisely matches with CuI thus negating the possibility of BioMOF formation. However, changes in the relative intensities of the different peaks hints that aspartic acid act as an capping agent which inhibits growth in all other planes except (111) plane. The results obtained from CD and Zeta potential measurements confirm the presence of amino acids on the surface. After performing various controlled reactions, it may be inferred that AA act as reducing agent under hydrothermal conditions. The thermal stability was analyzed with TGA which showed the material is stable upto 400 ºC. BET surface area analysis showed the value of 42.878 m^2g^{-1} with pore size diameter of 4.942 nm. Based on previous reports on the precursors used, CLA-16 was thought to behave as an enzyme-mimic. Therefore, different type of enzyme-mimic activities was checked. Surprisingly, LAA-capped CuI showed impressive peroxidase-like activity as it oxidizes TMB to form blue colored product. Quantitative determination of the activity was done using UV-Vis as OxTMB shows absorption band at 652nm. Various controls were performed to rule out the possibilities of precursors showing the activity. The results inferred that CLA-16 shows activity manifold higher than individual precursors. Steady-state kinetics experiments were performed which showed that catalyst follows Michaelis-Menten type kinetics for both TMB and H_2O_2. V_{max} and K_m of CLA-16 with H_2O_2 were found to be 0.00312 mM/min and 1.61515 mM respectively and for TMB values of V_{max} and K_m are 0.08563mM/min and 1.58295mM respectively. Further, effect of pH and temperature on stability and enzyme-mimicking behaviour of CLA-16 were examined. The catalyst showed highest activity at pH 4. CLA-16 microcrystals were stable even after 3 days in acidic and basic

pH buffers. With increase in temperature, activity of CLA-16 enhances significantly that makes it suitable for industrial applications. Due to heterogeneous nature of CLA-16, the catalyst can be easily recovered. The oxidation of TMB proceeds via OH radical as confirmed by the formation of fluorescent adduct with TA (λ_{em}=410 nm). It is obvious that synergistic effect of CuI and LAA in a near vicinity that enhances the peroxidase activity. Other than enzyme-mimic, CLA-16 shows orange coloured fluorescence in solid state. Similar to other CuI based materials, CLA-16 also shows solvatochromic behaviour. Apart from AA, other acidic, basic and neutral amino acids were also used as a capping agent to synthesize other samples using same synthesis procedure. Even other biomolecules such as ascorbic acid and citric acid that are well-known capping and reducing agent can also be used instead of amino acids to produce biomolecules-capped CuI materials. Interestingly, significant changes were observed in the morphologies. Changing the amino acid also affect the crystallinity as well as relative intensities of characteristic peaks in CuI. Therefore, it can be concluded that we have developed a new facile route to synthesize CuI microcrystals using APS as an oxidizing agent, amino acids as reducing as well as capping agents that can be used as a peroxidase-mimic in industrial applications.

Chapter 6

Future Work

Amino acids are well-explored as a capping agent in nanoparticle synthesis. In present case also, all spectroscopic evidences confirm that amino acid act as a capping agent and reducing agent. However, further experimental and theoretical studies are required to understand the complete mechanism from which CuI, APS and LAA interact to finally produce shiny CuI microcrystals. Single crystal XRD analysis is crucial to understand the arrangement of Copper and Iodine atoms in the unit cell as it can tune the photophysical properties such as fluorescence/phosphorescence. Photoluminescence property of CLA-16 is also needed to be studied thoroughly. These enzyme-mimics (peroxidase) can be used for sensing of important biomolecules such as glucose, glutathione, lactic acid *etc.* Other enzyme activities common for Cu-based materials can also be examined. Apart from AA, detailed spectroscopic and microscopic analysis is required for samples synthesized using other amino acids/biomolecules. Enzyme-mimic activity for all the samples needed to be checked and compared. As CuI is used in various applications. It is necessary to investigate the effect of amino acid capping on these activities of CuI, e.g. catalysis, thermoelectric, X-ray scintillators, fluorescent inks, optoelectronics, solar cell *etc.* These CuI crystals can also be used as precursors to fabricate perovskite materials that are of utmost importance in energy related applications.

References

(1) Yusuf, V. F.; Malek, N. I.; Kailasa, S. K. Review on Metal-Organic Framework Classification, Synthetic Approaches, and Influencing Factors: Applications in Energy, Drug Delivery, and Wastewater Treatment. *ACS Omega* **2022**, *7* (49), 44507–44531. https://doi.org/10.1021/acsomega.2c05310.

(2) Imaz, I.; Rubio-Martínez, M.; An, J.; Solé-Font, I.; Rosi, N. L.; Maspoch, D. Metal-Biomolecule Frameworks (MBioFs). *Chem. Commun.* **2011**, *47* (26), 7287–7302. https://doi.org/10.1039/c1cc11202c.

(3) Liu, J.; Li, Y.; Lou, Z. Recent Advancements in MOF/Biomass and Bio-MOF Multifunctional Materials: A Review. *Sustain.* **2022**, *14* (10), 1–17. https://doi.org/10.3390/su14105768.

(4) Quaresma, S.; André, V.; Antunes, A. M. M.; Vilela, S. M. F.; Amariei, G.; Arenas-Vivo, A.; Rosal, R.; Horcajada, P.; Duarte, M. T. Novel Antibacterial Azelaic Acid BioMOFs. *Cryst. Growth Des.* **2020**, *20* (1), 370–382. https://doi.org/10.1021/acs.cgd.9b01302.

(5) Damodaran, S. Amino Acids, Peptides, and Proteins. *Fennema's Food Chem.* **2017**, 235–356. https://doi.org/10.1201/9781315372914.

(6) Newar, R.; Akhtar, N.; Antil, N.; Kumar, A.; Shukla, S.; Begum, W.; Manna, K. Amino Acid-Functionalized Metal-Organic Frameworks for Asymmetric Base–Metal Catalysis. *Angew. Chemie - Int. Ed.* **2021**, *60* (19), 10964–10970. https://doi.org/10.1002/anie.202100643.

(7) Huang, Y.; Zhong, H.; Jiang, C.; Yang, J.; Zhang, J.; Zhao, F.; Liu, C. Copper-Based Nanomaterials as Peroxidase Candidates for Intelligent Colorimetric Detection and Antibacterial Applications. *Particuology* **2024**, *84*, 126–135. https://doi.org/10.1016/j.partic.2023.03.009.

(8) Troyano, J.; Zamora, F.; Delgado, S. Copper(i)-Iodide Cluster Structures as Functional and Processable Platform Materials. *Chem. Soc. Rev.* **2021**, *50* (7), 4606–4628. https://doi.org/10.1039/d0cs01470b.

(9) Liu, A.; Zhu, H.; Kim, M. G.; Kim, J.; Noh, Y. Y. Engineering Copper Iodide (CuI) for Multifunctional p-Type Transparent Semiconductors and Conductors. *Adv. Sci.* **2021**, *8* (14), 1–19. https://doi.org/10.1002/advs.202100546.

(10) Mohan, V.; Gautam, A. K.; Choudhary, S. D.; Mariam Bee, M. K.; Puviarasi, R.; Saranya, S.; Agrawal, N. Enhanced Performance Organic Light Emitting Diode with CuI:CuPC Composite Hole Transport Layer. *IEEE Trans. Nanotechnol.* **2020**, *19*, 699–703. https://doi.org/10.1109/TNANO.2020.3019096.

(11) Wang, S.; Wahiduzzaman, M.; Davis, L.; Tissot, A.; Shepard, W.; Marrot, J.; Martineau-Corcos, C.; Hamdane, D.; Maurin, G.; Devautour-Vinot, S.; Serre, C. A Robust Zirconium Amino Acid Metal-Organic Framework for Proton Conduction. *Nat. Commun.* **2018**, *9* (1), 1–8. https://doi.org/10.1038/s41467-018-07414-4.

(12) Mon, M.; Bruno, R.; Lappano, R.; Maggiolini, M.; Di Donna, L.; Ferrando Soria, J.; Armentano, D.; Pardo, E. A Biocompatible Aspartic-Decorated Metal-Organic Framework with Tubular Motif Degradable under Physiological Conditions. *Inorg. Chem.* **2021**, *60* (18), 14221–14229. https://doi.org/10.1021/acs.inorgchem.1c01701.

(13) Gizer, G.; Sahiner, M.; Yildirim, Y.; Demirci, S.; Can, M.; Sahiner, N. Rod-like L-Aspartic Acid-Cu(II) Metal Organic Frameworks; Synthesis, Characterization and Biomedical Properties. *Curr. Res. Green Sustain. Chem.* **2021**, *4* (May), 100110. https://doi.org/10.1016/j.crgsc.2021.100110.

(14) Liu, S.; Wu, X.; Xiong, J.; Yuan, X.; Zong, M. H.; Lou, W. Y. Aspartic Acid Based Metal-Organic Frameworks with Dual Function of NADH Peroxidase and Glycerol Dehydrogenase-Mimicking Activities. *Mater. Chem. Front.* **2022**, *6* (22), 3391–3401. https://doi.org/10.1039/d2qm00770c.

(15) Ravaro, L. P.; Mafud, A. C.; Li, Z.; Reinheimer, E.; Simone, C. A.; Mascarenhas, Y. P.; Ford, P. C.; de Camargo, A. S. S. New Emissive Mononuclear Copper (I) Complex: Structural and Photophysical Characterization Focusing on Solvatochromism, Rigidochromism and Oxygen Sensing in Mesoporous Solid Matrix. *Dye. Pigment.* **2018**, *159* (I), 464–470.

https://doi.org/10.1016/j.dyepig.2018.07.020.

(16) Wang, J. J.; Chen, C.; Chen, W. G.; Yao, J. S.; Yang, J. N.; Wang, K. H.; Yin, Y. C.; Yao, M. M.; Feng, L. Z.; Ma, C.; Fan, F. J.; Yao, H. Bin. Highly Luminescent Copper Iodide Cluster Based Inks with Photoluminescence Quantum Efficiency Exceeding 98%. *J. Am. Chem. Soc.* **2020**, *142* (8), 3686–3690. https://doi.org/10.1021/jacs.9b12908.

(17) Almasoudi, M.; Saeed, A.; Salah, N.; Alshahrie, A.; Hasan, P. M. Z.; Melaibari, A.; Koumoto, K. CuI: A Promising Halide for Thermoelectric Applications below 373 K. *ACS Appl. Energy Mater.* **2022**, *5* (8), 10177–10186. https://doi.org/10.1021/acsaem.2c01929.

(18) Li, J.; Wang, R.; Zhang, D.; Su, Z.; Li, H.; Yan, Y. Copper Iodide (CuI) Coating as a Self-Cleaning Adsorbent for Highly Efficient Dye Removal. *J. Alloys Compd.* **2019**, *774*, 191–200. https://doi.org/10.1016/j.jallcom.2018.09.373.

(19) Pramanik, A.; Laha, D.; Bhattacharya, D.; Pramanik, P.; Karmakar, P. A Novel Study of Antibacterial Activity of Copper Iodide Nanoparticle Mediated by DNA and Membrane Damage. *Colloids Surfaces B Biointerfaces* **2012**, *96*, 50–55. https://doi.org/10.1016/j.colsurfb.2012.03.021.

(20) Li, H.; Liu, T.; Wei, P.; Lin, L.; Gao, D.; Wang, G.; Bao, X. High-Rate CO 2 Electroreduction to C 2+ Products over a Copper-Copper Iodide Catalyst . *Angew. Chemie* **2021**, *133* (26), 14450–14454. https://doi.org/10.1002/ange.202102657.

(21) Yang, Y.; Gong, Y.; Li, X.; Li, M.; Wei, Q.; Zhou, B.; Zhang, J. Alkaline-Stable Peroxidase Mimics Based on Biological Metal-Organic Frameworks for Recyclable Scavenging of Hydrogen Peroxide and Detecting Glucose in Apple Fruits. *ACS Sustain. Chem. Eng.* **2022**, *10* (32), 10685–10698. https://doi.org/10.1021/acssuschemeng.2c03184.

(22) Jain, S.; Sharma, B.; Thakur, N.; Mishra, S.; Sarma, T. K. Copper Pyrovanadate Nanoribbons as Efficient Multienzyme Mimicking Nanozyme for Biosensing Applications. *ACS Appl. Nano Mater.* **2020**, *3* (8), 7917–7929. https://doi.org/10.1021/acsanm.0c01415.

(23) Wu, Z. F.; Wang, Z.; Zhang, Y.; Ma, Y. L.; He, C. Y.; Li, H.; Chen, L.; Huo, Q. S.; Wang, L.; Li, Z. Q. Amino Acids-Incorporated Nanoflowers with an Intrinsic Peroxidase-like Activity. *Sci. Rep.* **2016**, *6* (March), 1–7. https://doi.org/10.1038/srep22412.

(24) Abdolmohammadi, S.; Afsharpour, M. An Operationally Simple Green Procedure for the Synthesis of Dihydropyrimido[4,5-d] Pyrimidinetriones Using CuI Nanoparticles as a Highly Efficient Catalyst. *Zeitschrift fur Naturforsch. - Sect. B J. Chem. Sci.* **2015**, *70* (3), 171–176. https://doi.org/10.1515/znb-2014-0207.

(25) Yu, J. C.; Zhao, F. G.; Shao, W.; Ge, C. W.; Li, W. S. Shape-Controllable and Versatile Synthesis of Copper Nanocrystals with Amino Acids as Capping Agents. *Nanoscale* **2015**, *7* (19), 8811–8818. https://doi.org/10.1039/c5nr00146c.

(26) Bilal, M.; Khaliq, N.; Ashraf, M.; Hussain, N.; Baqar, Z.; Zdarta, J.; Jesionowski, T.; Iqbal, H. M. N. Enzyme Mimic Nanomaterials as Nanozymes with Catalytic Attributes. *Colloids Surfaces B Biointerfaces* **2023**, *221* (October 2022), 112950. https://doi.org/10.1016/j.colsurfb.2022.112950.

(27) Gao, L.; Zhuang, J.; Nie, L.; Zhang, J.; Zhang, Y.; Gu, N.; Wang, T.; Feng, J.; Yang, D.; Perrett, S.; Yan, X. Intrinsic Peroxidase-like Activity of Ferromagnetic Nanoparticles. *Nat. Nanotechnol.* **2007**, *2* (9), 577–583. https://doi.org/10.1038/nnano.2007.260.

(28) Liu, F.; He, J.; Zeng, M.; Hao, J.; Guo, Q.; Song, Y.; Wang, L. Cu–Hemin Metal-Organic Frameworks with Peroxidase-like Activity as Peroxidase Mimics for Colorimetric Sensing of Glucose. *J. Nanoparticle Res.* **2016**, *18* (5), 1–9. https://doi.org/10.1007/s11051-016-3416-z.

(29) Wang, S.; Deng, W.; Yang, L.; Tan, Y.; Xie, Q.; Yao, S. Copper-Based Metal-Organic Framework Nanoparticles with Peroxidase-Like Activity for Sensitive Colorimetric Detection of Staphylococcus Aureus. *ACS Appl. Mater. Interfaces* **2017**, *9* (29), 24440–24445. https://doi.org/10.1021/acsami.7b07307.

(30) Dutta, A. K.; Das, S.; Samanta, S.; Samanta, P. K.; Adhikary, B.; Biswas, P. CuS

Nanoparticles as a Mimic Peroxidase for Colorimetric Estimation of Human Blood Glucose Level. *Talanta* **2013**, *107*, 361–367. https://doi.org/10.1016/j.talanta.2013.01.032.

(31) Chen, W.; Chen, J.; Liu, A. L.; Wang, L. M.; Li, G. W.; Lin, X. H. Peroxidase-Like Activity of Cupric Oxide Nanoparticle. *ChemCatChem* **2011**, *3* (7), 1151–1154. https://doi.org/10.1002/cctc.201100064.

(32) Qin, F. X.; Jia, S. Y.; Wang, F. F.; Wu, S. H.; Song, J.; Liu, Y. Hemin@metal-Organic Framework with Peroxidase-like Activity and Its Application to Glucose Detection. *Catal. Sci. Technol.* **2013**, *3* (10), 2761–2768. https://doi.org/10.1039/c3cy00268c.

(33) Huitorel, B.; Utrera-Melero, R.; Massuyeau, F.; Mevelec, J. Y.; Baptiste, B.; Polian, A.; Gacoin, T.; Martineau-Corcos, C.; Perruchas, S. Luminescence Mechanochromism of Copper Iodide Clusters: A Rational Investigation. *Dalt. Trans.* **2019**, *48* (22), 7899–7909. https://doi.org/10.1039/c9dt01161g.

(34) Park, G.; Yang, H.; Kim, T. H.; Kim, J. Copper(I) Coordination Polymers of N,N/-Bis[3-(Methylthio)Propyl] Pyromellitic Diimide: Crystal Transformation and Solvatochromism by Halogen-π Interactions. *Inorg. Chem.* **2011**, *50* (3), 961–968. https://doi.org/10.1021/ic101562p.

Supporting Information-

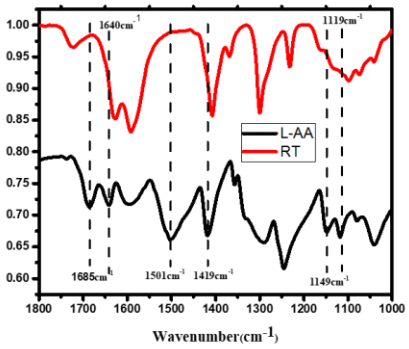

Figure (a) *FT-IR spectra of L-Aspartic acid and RT BioMOF.*

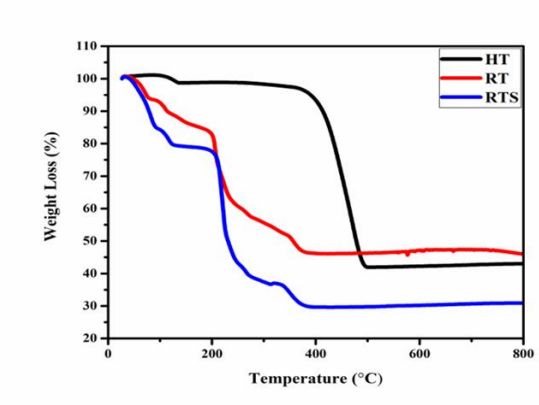

Figure (b) *TGA curve of RT, RTS and CLA-16 in N_2 environment.*

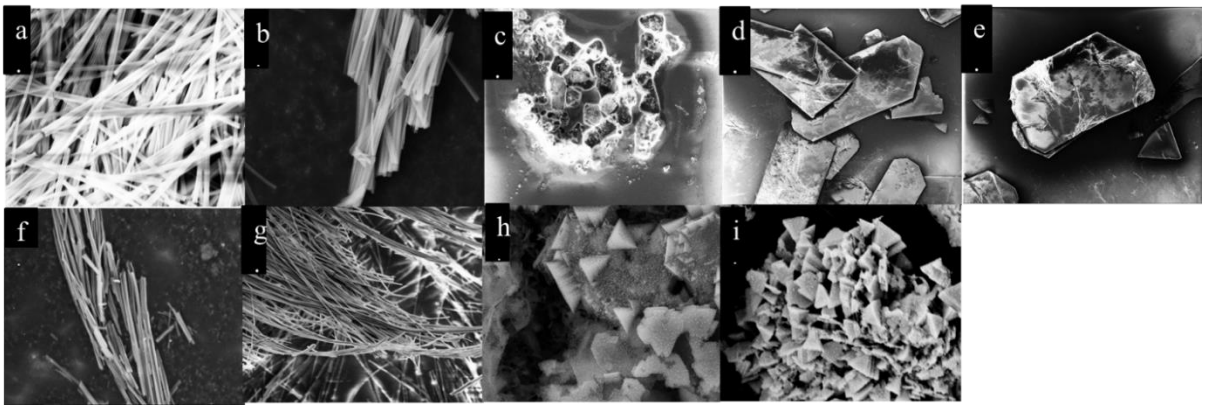

Figure (c) *FE-SEM images of (a)* 10 mM APS (b) 25 mM APS (c) CuI (stir) (d&e) LAA:CuI (3:1) (f) L-AA and H_2O_2 (g) CuCO3 (h) DMSO:water (1:4)

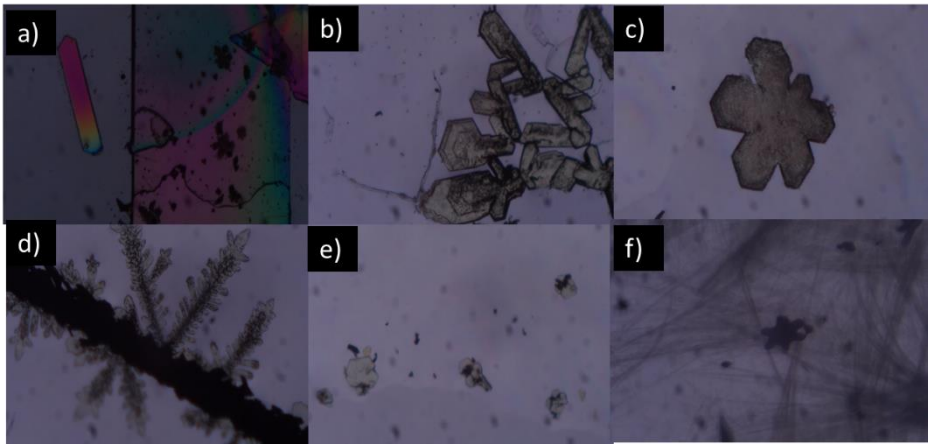

Figure (d) *POM images* (a & b) LAA:CuI (2:1) (c & d) LAA:CuI (3:1) (e) LAA:CuI (1:2) (f) RTS

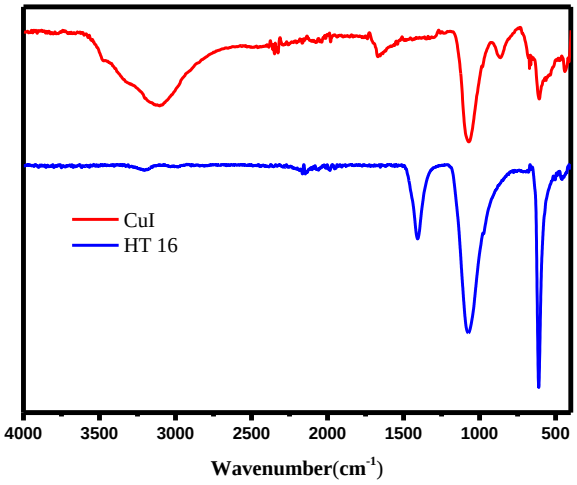

Figure (e) *FT-IR spectra of CuI and CLA-16.*

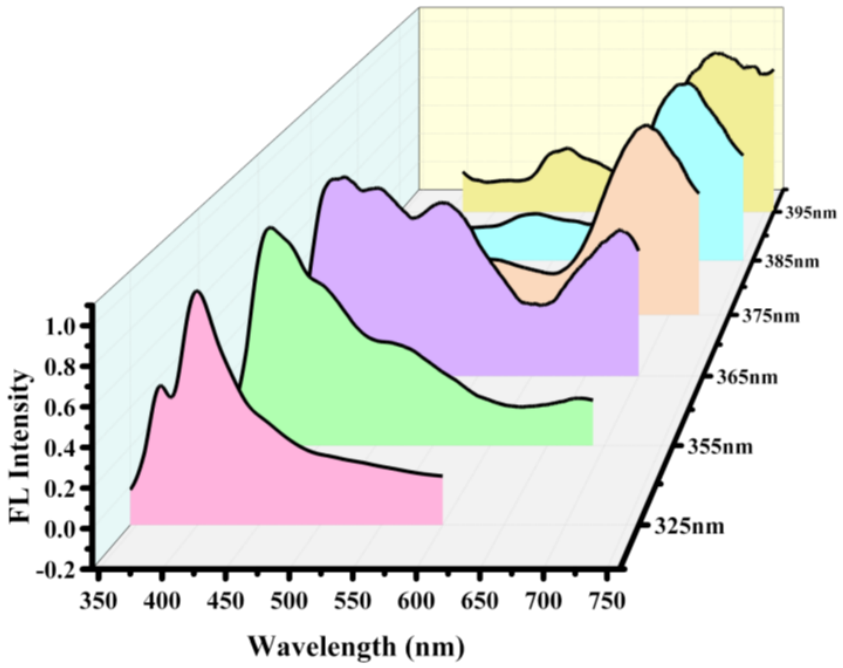

Figure (f) *Fluoroscence spectra of CLA-16 in liquid form (water) at different wavelengths.*

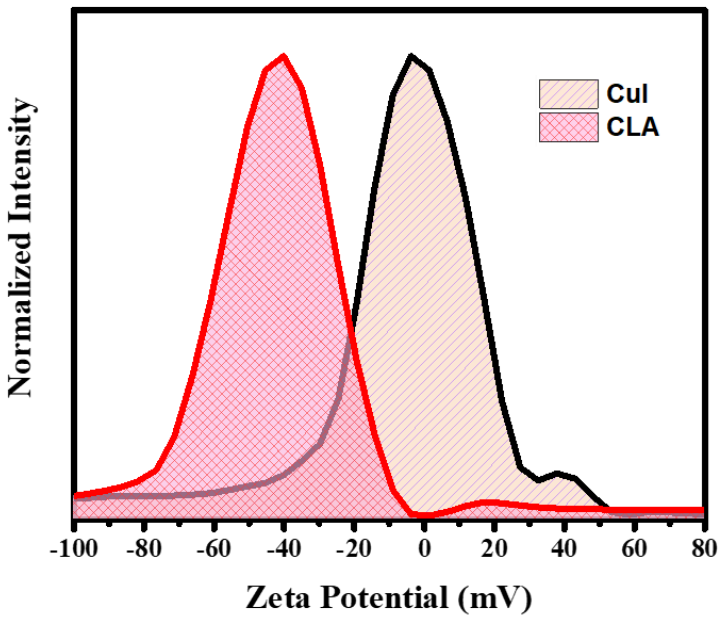

Figure (g) *Change in Zeta potential of CuI before and after (CLA-16) synthesis*

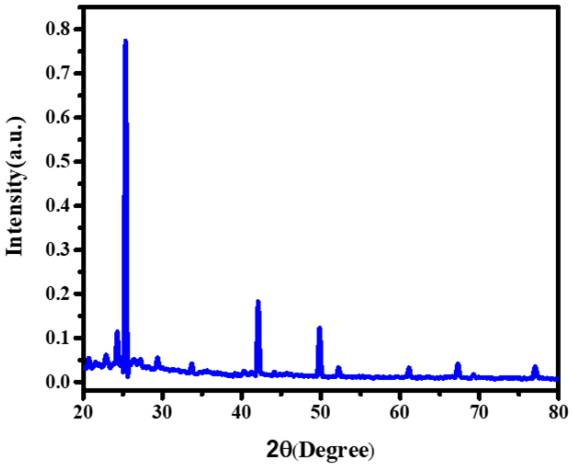

Figure (h) *PXRD data of CLA-16 after one catalytic cycle.*